



Reframing gullies as recharge zones in dryland landscapes of the Loess Plateau, China

Zhenxia Ji^{1,2,3,4}, Alan D. Ziegler⁵, and Li Wang^{1,2,3,4}

¹State Key Laboratory of Soil and Water Conservation and Desertification Control,

College of Natural Resources and Environment, Northwest A&F University, Yangling 712100, China

²College of Soil and Water Conservation Science and Engineering, Northwest A&F University, Yangling 712100, China

³State Key Laboratory of Soil and Water Conservation and Desertification Control, Chinese Academy of Sciences, the Ministry of Water Resources, Yangling 712100, China

⁴Institute of Soil and Water Conservation, Chinese Academy of Sciences and the Ministry of Water Resources, Yangling 712100, China

⁵Andaman Coastal Station for Research and Development, Kasetsart University, Ranong, Thailand

Correspondence: Li Wang (wangli5208@nwsuaf.edu.cn)

Received: 20 August 2025 – Discussion started: 24 September 2025

Revised: 28 February 2026 – Accepted: 25 March 2026 – Published: 9 April 2026

Abstract. Large gullies in dryland landscapes are often indicators of land degradation by surface runoff. However, under conditions where gully systems are hydrologically arrested by restoration interventions that increase water residence time – most notably check dams and ponds – they may also function as hydrologically active zones of groundwater recharge and subsurface connectivity. In China’s Loess Plateau, we assess these functions in the Nianzhuang Catchment using a multi-indicator, process-based approach that integrates stable isotopes ($\delta^2\text{H}$, $\delta^{18}\text{O}$), chloride concentrations, and groundwater level fluctuations. Our results show that precipitation is the dominant source of recharge for shallow pore water within engineered gully zones, while deeper fissure water is replenished more slowly through percolation. Hydrological arrest through ecological engineering interventions acts as focal points for groundwater infiltration, enhancing recharge in otherwise limited dryland systems. Estimated annual recharge in the monitored gully-zone pore aquifer (238–241 mm) is equivalent to about 43 % of the mean annual precipitation at the site, a site-specific recharge magnitude that far exceeds reported catchment-wide recharge rates observed in nearby tableland and hilly areas. Our results indicate that engineered gully systems can act as focused recharge zones rather than solely degraded landforms. By linking runoff convergence and ponding to measurable recharge responses, the study provides a process-

based framework for assessing groundwater dynamics in managed semi-arid landscapes.

1 Introduction

Groundwater recharge is a critical yet poorly understood component of hydrological cycles in dryland catchments (Li et al., 2024a). It is shaped by the precipitation regime, surface landcover heterogeneity, integrity of the subsurface regolith, characteristics of the underlying bedrock, and human interventions (De Vries and Simmers, 2002; Owuor et al., 2016; Salek et al., 2018; Xu and Beekman, 2019; Zhang et al., 2020; Li et al., 2024b; Medici et al., 2024). While favorable subsurface flow pathways can locally enhance recharge, dryland regions are highly sensitive to even slight changes in precipitation, soil moisture, or runoff generation. This heightened sensitivity reflects their position along climatic ecotones and the influence of complex land–atmosphere–biosphere feedbacks (Kuang et al., 2019; Al-Oqaili et al., 2020; He et al., 2020; Jin et al., 2019; Jia et al., 2024). Small changes in these processes can cascade across catchments at various scales, amplifying existing vulnerabilities to ecological and social systems (Nicholson, 2011; Huang et al., 2017; Berg et al., 2016). In these fragile landscapes, understanding groundwater replenishment processes is crucial for sus-

taining ecosystems, securing water, and guiding restoration and management (Gleeson et al., 2016; Jasechko and Perrone, 2021; Scanlon et al., 2002).

Despite a growing body of research on groundwater recharge in (semi-) arid regions, significant knowledge gaps remain in landscapes with pronounced spatial heterogeneity, such as slopes, hilltops, and gully systems, where infiltration pathways and recharge processes can diverge sharply over short distances (Tooth, 2012; Manna et al., 2019; Letz et al., 2021). Gully systems, often seen as signs of land degradation, may beneficially act as recharge zones, capturing and infiltrating surface runoff during episodic rainfall (Tan et al., 2017; Li et al., 2024a; Xue et al., 2025). This same topographic focusing enables the rapid downslope transport of contaminants, including agricultural nutrients, sediments, and associated pollutants (Lian et al., 2025; Qu et al., 2025). However, the role of gullies in promoting vertical infiltration into groundwater is highly dependent on local subsurface connectivity and permeability conditions. Moreover, their broader hydrological functions remain poorly quantified, especially under the influence of widespread human interventions such as check dams and artificial ponds. While these structures are typically designed to arrest land surface degradation, they can substantially alter surface–subsurface connectivity and reshape recharge dynamics in uncertain ways (Lamontagne et al., 2021; Huang et al., 2019; Wang et al., 2023).

Worldwide, loess covers approximately 6% of the land surface area, forming discontinuous east–west belts in the mid-latitude forest-steppe, steppe, and desert-steppe zones of both hemispheres (Liu, 1985; Pécsi, 1990; Li et al., 2020). Among these, the Chinese Loess Plateau, the focus of our study accounts for approximately 7.4% of the global loess area (635 280 km²; Li et al., 2020). It serves as a globally important natural laboratory for studying soil erosion and groundwater recharge processes, due to its exceptionally thick loess deposits (Li et al., 2021), highly erodible soils, intense summer rainstorms, and long history of agricultural activity, which collectively make it one of the most severely eroded regions worldwide (Shi and Shao, 2000; Fu et al., 2011). Its distinctive stratigraphic structure, characterized by thick, low-permeability loess layers, fundamentally governs groundwater behavior (Qiao et al., 2017). Meanwhile, extensive human interventions aimed at erosion control, including large-scale afforestation and gully engineering projects, have profoundly altered regional hydrological processes and the spatial redistribution of water (Wang et al., 2020; Zhao et al., 2024).

The setting for our investigation is a semi-arid landscape that has been shaped by severe soil erosion, extensively modified by engineered landforms; and it is now characterized by chronic water scarcity (Fu et al., 1999; Liu et al., 2017; Liu and Li, 2017; Li et al., 2021; Huang et al., 2024). Water scarcity manifests as declining groundwater levels, reduced streamflow, dried-up wells and springs, and limited irrigation

capacity (Yu et al., 2025). In such vulnerable environments, understanding the sources and sustainability of groundwater recharge is critical for long-term water resource management (Ajjur and Baalousha, 2021; Meles et al., 2024). Groundwater, for example, is a lifeline for rural communities in the hilly–gully region, yet scientific attention has largely bypassed the gullies themselves. Most previous studies have focused on recharge processes in tablelands and loess-covered hills, highlighting slow “piston flow” as the dominant mechanism (Huang and Pang, 2011; Huang et al., 2013; Li et al., 2017; Lu, 2020; Wang et al., 2024). However, the deep-profile recharge mechanisms observed in these areas may not apply to the gully-dominated landscapes of the Loess Plateau (Wang et al., 2024; Qiao et al., 2017; Zhu et al., 2018). Moreover, the hydrological functions of widely distributed gully systems, especially under the influence of engineering structures such as check dams, remain insufficiently quantified, and their underlying processes have long remained in the research shadow (Liu et al., 2011).

Therefore, this study selects the Nianzhuang Catchment, a typical gully area on the Loess Plateau impacted by check dams, to establish a multi-method framework for assessing groundwater recharge by integrating stable isotope analysis ($\delta^2\text{H}$ and $\delta^{18}\text{O}$), chloride concentrations, water table fluctuations, and hydro-statistical modeling. Specifically, our goals are to: (1) characterize the isotopic and hydrochemical signatures of precipitation, surface water (ponds), shallow pore water, and deeper fissure water; (2) identify and trace hydraulic connections and flow paths of different water bodies; and (3) quantitatively estimate pore-water recharge rates. This integrated approach aims to advance understanding of groundwater dynamics in complex dryland terrains, reframes engineered gully systems as critical recharge zones in engineered dryland landscapes, providing actionable insights for sustainable groundwater management and ecological restoration in the Loess Plateau and similar semi-arid regions worldwide.

2 Sampling site

The Nianzhuang Catchment is located northwest of Yan’an City in Shaanxi Province, China (approximately 36°42′ N, 109°31′ E). As a tributary of the Yan River, which ultimately flows into the Yellow River, the catchment spans 53.94 km² and includes the well-studied Yangjuangou sub-catchment (3.11 km²; ~ 36°35′ N, ~ 109°32′ E), previously investigated in numerous hydrological and ecological studies (Fu et al., 1999, 2011, 2017; Liu and Li, 2017). Elevation ranges from 896 to 1269 m, with terrain gradually sloping from northwest to southeast (Fig. 1). The region experiences a semi-arid continental monsoon climate, with a mean annual precipitation of approximately 550 ± 100 mm, concentrated between July and September (Liu et al., 2017).

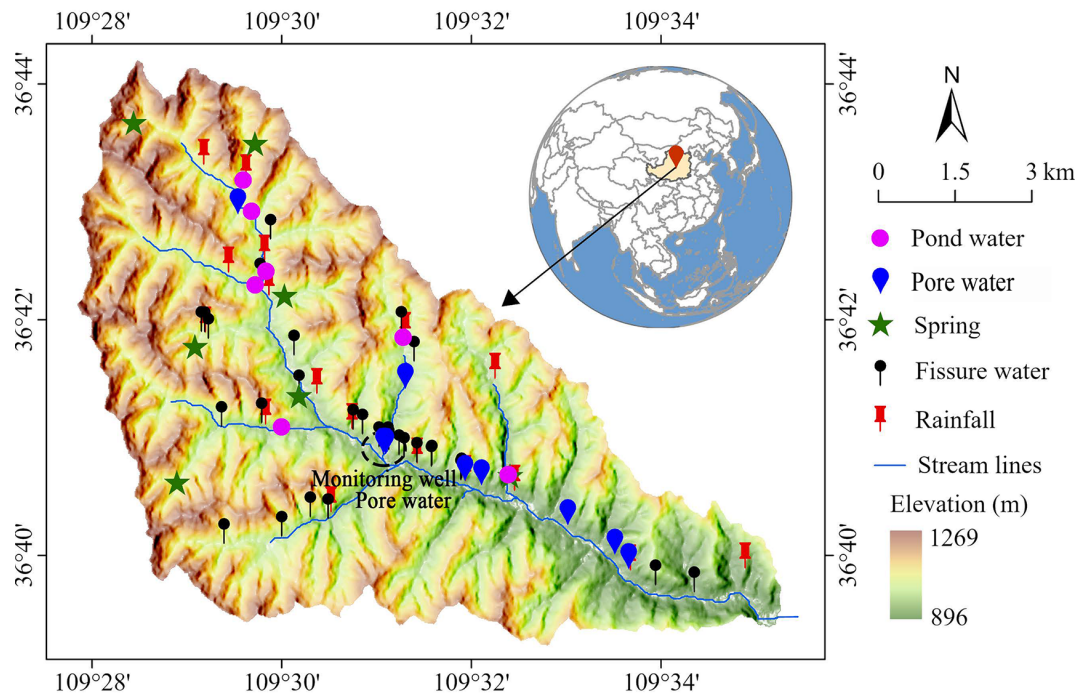


Figure 1. The geographical location and sampling sites for rainfall, pond water, pore water, spring water, and fissure water in the Nianzhuang Catchment. The Nianzhuang Catchment is located in the hilly and gully region of the central Loess Plateau, with elevations ranging from 896 to 1269 m. The average depth of pore water wells is 8.0 ± 1.5 m (range: 4–10 m), while that of fissure water wells is 57.6 ± 29.2 m (range: 25–170 m). These sampling sites represent locations where both rainy and dry season samples were collected, and are all situated within the gully areas of the catchment.

The catchment features highly dissected loess terrain, with characteristic soils and landforms such as Loess Liang (ridges), Loess Mao (mounds), and steep loess slopes (Cai et al., 2019). Gullies, often “V”- or “U”-shaped, dominate the lower-lying regions and serve as important recharge zones. These landforms, together with ancient landslides, minor collapses, and sinkholes, highlight the geomorphic instability of the Loess Plateau landscape (Li et al., 2021). From May to October 2023, total rainfall reached 420 mm, with 115 mm in September alone. Despite this substantial precipitation, field observations revealed shallow infiltration depths on loess slopes even after heavy rainfall events of up to 41 mm. Infiltration was limited to 20–30 cm at hilltops and about 80 cm at mid-slope, with no distinct preferential flow and largely unsaturated soil profiles (Fig. 2). These observations suggest that groundwater recharge occurs mainly through surface or near-surface runoff converging into engineered gully systems, underscoring their critical role as focused zones of groundwater recharge and key sites for studying these processes.

The stratigraphy of the catchment reflects the typical layered structure of the Loess Plateau, which plays a key role in controlling groundwater recharge. In upland hilly areas, thick loess deposits overlie bedrock, with the Upper Pleistocene Malan Loess, a light grayish-yellow, loosely textured,

and silt-rich unit (> 60 %), characterized by well-developed vertical joints and abundant hematite and goethite. Beneath it lies the Middle Pleistocene Lishi Loess, a grayish-yellow to light brown unit with prominent jointing and higher iron mineral content. Below the loess, the Neogene Red Clay appears as a distinctly reddish, calcareous nodule-bearing aquitard due to its low permeability. The entire sequence rests on Jurassic sandstone–conglomerate bedrock, composed mainly of quartz-rich fluvial–lacustrine deposits.

Loess thickness in the Liang and Mao regions often exceeds 150 m, resulting in deep water tables and limited groundwater accessibility. In contrast, gully zones exhibit distinctly different hydrogeological characteristics. Here, thinner loess layers overlie Neogene and Jurassic formations, sometimes interbedded with coal seams up to 5 m thick (Fig. 3a–c). The significant reduction in loess thickness, combined with the relatively high permeability of Neogene coarse sandstone and conglomerate ($0.07\text{--}0.31\text{ m d}^{-1}$), creates favorable conditions for infiltration and focused recharge. These dynamics are especially evident at gully heads, where surface runoff from adjacent uplands converges and infiltrates, forming efficient recharge zones. As a result, gully areas tend to have shallower water tables and more rapid water renewal, making them more suitable for domestic groundwater use. Springs frequently emerge at gully bottoms

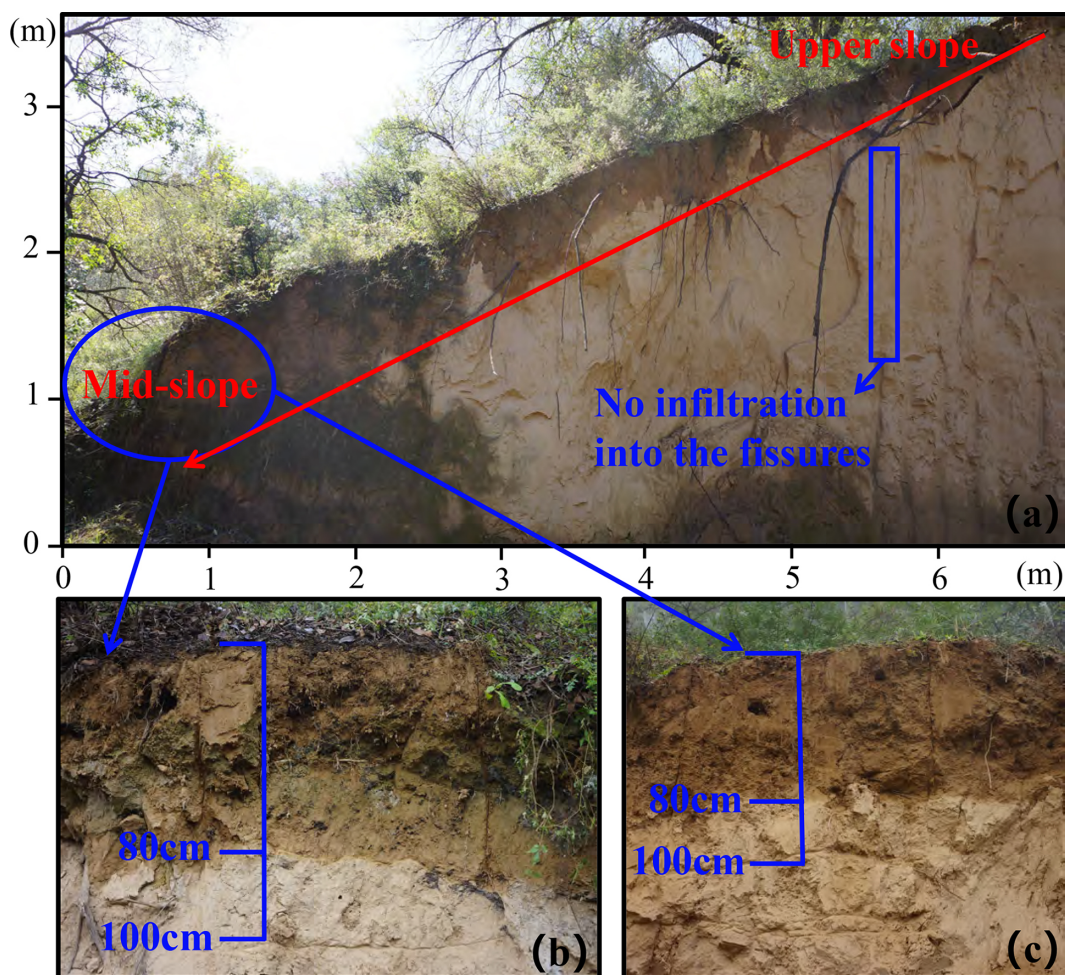


Figure 2. The topographic profile of the Nianzhuang Catchment in the hilly region of the Loess Plateau. Full profile from the top to mid-slope (a); two repeated mid-slope profiles (b, c). The photo was taken after a 41 mm rainfall event over 4 d. Subsequent measurements showed that infiltration depths reached only 20–30 cm at the top of the slope, compared to approximately 80 cm at the mid-slope positions.

where lateral flow is facilitated at the loess–bedrock interface. Streams in this dry environment are largely intermittent.

Groundwater in the catchment can be broadly categorized into three types: pore water, spring water, and fissure water. Pore water is stored in permeable sandstone and conglomerate aquifers beneath loess and above mudstone or red clay. These aquifers are approximately 2–3 m thick, exhibit a sheet-like distribution, and have low water yield. Conceptually, “pore water” here refers to groundwater in a saturated aquifer, not to soil moisture. Fissure water occurs in fractured bedrock aquifers, which are spatially discontinuous due to irregular fracture development. The main water-bearing zones include cavities and jointed fissure networks, with an average aquifer thickness of about 6 m and moderate water yield. Hydraulic conductivity in these sandstone and conglomerate aquifers ranges from 0 to 0.47 m d^{-1} (Cai et al., 2019). Spring water emerges primarily at gully bases, especially in upper catchments, and originates from both pore and fissure sources, possibly supplemented by surface or pond water.

Springs fed by pore water typically have low discharge rates ($0\text{--}0.1 \text{ L s}^{-1}$) and low water yield, while those fed by fissure water exhibit moderate discharge rates ($0.5\text{--}1.0 \text{ L s}^{-1}$) and moderate water yield.

Over recent decades, landscape rehabilitation through the Grain for Green Project and land reshaping under the Gully Land Consolidation Project have significantly altered the hydrological regime (Fu et al., 1999; Liu et al., 2017). Historically, surface runoff in the degraded catchment was flashy and episodic due to sparse vegetation. However, ecological restoration and small-scale engineering interventions, such as check dams, terraces, roads, and ponds, have moderated surface hydrology. Surface runoff, generated primarily during storm events, now contributes alongside delayed baseflow from groundwater recharge and interflow. The latter is often limited by the thick unsaturated zone in upland loess areas but may be enhanced in gully regions, where stratigraphy and land use favor infiltration (Wang et al., 2024; Gates et al., 2011). Gully areas also contain numerous check dams

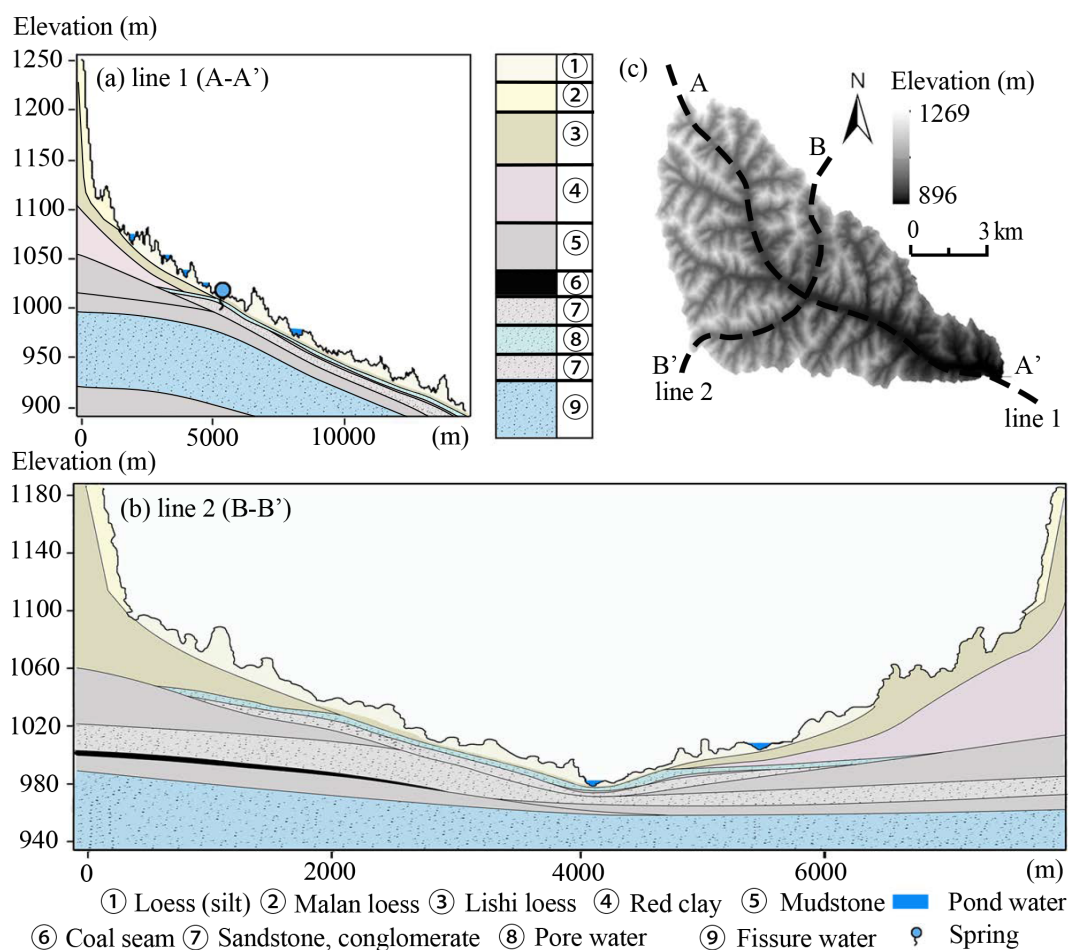


Figure 3. Hydrogeologic cross-section of the study area. Cross-section along Line 1 (Northwest–Southeast) (a); cross-section along Line 2 (Southwest–Northeast) (b); location map of Line 1 and Line 2 within the study area (c). The Malan Loess (11.7–12.6 Ka BP) and Lishi Loess (12.6–78.1 Ka BP) are two major Quaternary loess stratigraphic units in China. Based on hydrogeological research, the stratigraphy of the hilly region features a multi-layer structure from top to bottom: Upper Pleistocene Malan Loess, Middle Pleistocene Lishi Loess, Neogene Red Clay and Mudstone (2.58–23.03 Ma BP), and Jurassic Sandstone and Conglomerate (145–201.3 Ma BP). In the gully region, the stratigraphy includes Holocene loess (silt, 11.7 ka BP–present), Middle Pleistocene Lishi Loess, Neogene sandstone and mudstone, and Jurassic sandstone and conglomerate, with some areas containing coal seams up to 5 m thick.

and ponds, with most water sourced from Hortonian overland flow of slope lands and direct rainfall. These small water bodies, often constructed for erosion control and water retention, influence local hydrological dynamics and may play a role in enhancing infiltration and recharge.

3 Methods

Our approach integrates stable isotope analysis ($\delta^2\text{H}$ and $\delta^{18}\text{O}$), chloride concentration analysis, and water table fluctuation monitoring to investigate groundwater recharge dynamics. The isotopic composition of water bodies reflects both their origins and the processes they undergo, such as evaporation, infiltration, and mixing (Wan and Liu, 2016; Kumar et al., 2019; Dasgupta et al., 2024). Precipitation,

surface water, and groundwater typically exhibit distinct isotopic signatures due to these differing pathways (Gleeson et al., 2016; Kuang et al., 2019; Al-Oqaili et al., 2020). When isotopic patterns among water sources converge, it often indicates strong hydrological connectivity (Yang and Wang, 2023). Because stable isotopes behave conservatively, they serve as effective tracers of water sources and flow paths (Gleeson et al., 2016; Al-Oqaili et al., 2020; Dasgupta et al., 2024). In parallel, water table fluctuation (WTF) monitoring provides a means of estimating recharge by observing changes in groundwater levels in response to precipitation events (Nachabe, 2002; Heppner and Nimmo, 2005; Gumuła-Kawęcka et al., 2022). By combining these complementary methods, this study aims to elucidate groundwater recharge pathways and quantify recharge rates in gully regions, thereby identifying key recharge zones and advanc-

ing our understanding of groundwater processes in the Loess Plateau.

3.1 Field measurements of hydrological data

Precipitation was collected from 24 October 2023, to 24 October 2024, using a weather station situated in an open field within the catchment. Continuous groundwater level data were recorded from 24 September 2023, to 20 December 2024. Groundwater pressure and temperature were monitored using Onset HOBO U20-001-03 sensors (20 m range), with a pressure accuracy of $\pm 0.3\%$ FS (± 2.55 kPa) and a resolution of < 0.085 kPa, and a temperature accuracy of ± 0.44 °C with a resolution of 0.1 °C. The sensor was calibrated to atmospheric pressure before installation to ensure accurate measurement of absolute static water pressure, and water table levels were calculated based on the measured pressure data. The conversion relationship between water pressure and groundwater level is given by $Y = 0.86 \times X - 22.1$ where Y represents the groundwater level and X represents the water pressure. The conversion between water pressure and groundwater level is based on the principle of hydrostatics. The hydrostatic pressure P at the sensor is related to the height of the overlying water column h by $P = \rho gh$, where ρ is the water density and g is the gravitational acceleration. In unconfined aquifer, the pressure measured by the sensor corresponds directly to the static pressure exerted by the overlying water column. From this, the water column height h can be calculated, and combined with the sensor's installation elevation, the depth to the groundwater table can be determined. Notably, the monitoring well is located in the pore water layer of the gully region. The well is hand-dug (1.1 m wide, 10 m deep) and is unaffected by human activities.

Soil physical properties were assessed using the cutting ring method, based on undisturbed soil cores collected at five depth intervals: 0–10, 10–20, 20–30, 30–40, and 40–50 cm. Quadruplicate samples were taken near groundwater monitoring wells in the gully using pre-weighed cutting cylinders. The samples were immediately transported to the laboratory for analysis. Bulk density, capillary porosity, non-capillary porosity, total porosity, and field water capacity were determined following the LY/T 1215-1999 standard for forest soil water-physical properties. Soil particle size distribution was analyzed using a laser particle size analyzer at the College of Natural Resources and Environment, Northwest A&F University. Soil texture classification followed the USDA system: sand (0.05–2 mm), silt (0.002–0.05 mm), and clay (< 0.002 mm).

3.2 Water sampling

A total of 181 water samples were collected from various locations in rainy season (September 2023, 99 samples) and dry season (April 2024, 82 samples); see Fig. 1. Rainy season

samples included 48 from rainfall, 7 from pond water (water retention reservoirs), 9 from spring water, 9 from pore water, and 26 from fissure water. During the dry season, samples included 31 from rainfall, 6 from pond water, 8 from pore water, 29 from fissure water, and 8 from spring water.

Pore water was collected from several shallow, hand-dug wells measuring approximately 1.1 m in diameter and 4–10 m in depth. Fissure water was sampled from deeper, narrow-diameter wells (0.2 m wide, 25–170 m deep). In areas with numerous deep wells, we employed random sampling to ensure representative coverage of fissure water sources. To minimize the risk of collecting stagnant water, all pore and fissure water wells were purged for 10–15 min prior to sampling. Spring water was collected directly from natural discharge points, although most springs in the region exhibit low flow rates, typically less than 0.1 L s^{-1} , occasionally reaching up to 0.2 L s^{-1} .

A total of 18 bulk rainfall collectors were randomly and evenly distributed across the 54 km^2 study area, and samples were collected immediately following rainfall events. For nighttime precipitation, samples were collected the next morning at 06:00 a.m. LT (local time). During the study period, we collected two types of precipitation samples: (1) spatial samples from individual events (18 in the rainy season and 15 in the dry season) across the catchment, capturing spatial variability; and (2) sequential events at a fixed station (30 in the rainy season and 16 in the dry season), characterizing seasonal inputs.

During sampling, 100 mL collection bottles were rinsed two to three times with the sample water, then slowly filled to minimize air exposure. After filling, the bottles were tightly sealed with screw caps and further secured with Parafilm to prevent evaporation and contamination. All samples were immediately stored in a portable cooler at 4 °C and transported to the laboratory for isotopic and chloride concentration analysis.

3.3 Isotopic analysis

The $\delta^2\text{H}$ and $\delta^{18}\text{O}$ values of the water samples were determined using a Los Gatos Research liquid water isotope analyzer (Model 912-0032, LGR Inc., California, USA) at the Institute of Water-Saving Agriculture in Arid Areas of China, Northwest A&F University. Each sample was injected six times in the following sequence: three standard injections, followed by six natural sample injections, and then three additional standard injections. The isotope ratios were calculated using the average composition from injections 4 through 6.

Isotope values are expressed in delta (δ) notation, which represents the relative difference in isotope ratio between a sample and the Vienna Standard Mean Ocean Water (VSMOW) reference. The measurement precision was $\pm 0.5\%$ for $\delta^2\text{H}$ and $\pm 0.1\%$ for $\delta^{18}\text{O}$. The delta values were calcu-

lated using the following equations:

$$\delta^{18}\text{O} = \left(\frac{R_{\text{sample}}}{R_{\text{standard}}} \right) - 1 \quad (1)$$

$$\delta^2\text{H} = \left(\frac{R_{\text{sample}}}{R_{\text{standard}}} \right) - 1 \quad (2)$$

where R_{sample} and R_{standard} are the ratios of heavy to light isotopes ($^{18}\text{O}/^{16}\text{O}$ or $^2\text{H}/^1\text{H}$) in the sample and the standard, respectively. Results are expressed in per mil (‰).

3.4 Mixing process of different water bodies

Inverse transit time proxies (ITTPs) were calculated to assess differences in water transit times and mixing processes across various water bodies (Tetzlaff et al., 2009). ITTPs are defined as the ratio of the standard deviation of $\delta^{18}\text{O}$ in the water sample (e.g., pond water, spring water, pore water, or fissure water) to that in precipitation over the same time period:

$$\text{ITTP} = \frac{\sigma \delta^{18}\text{O}(\text{sample})}{\sigma \delta^{18}\text{O}(\text{precipitation})} \quad (3)$$

This ratio captures the attenuation of seasonal isotopic variability in $\delta^{18}\text{O}$ as water moves through the landscape. In general, ITTP values less than 1 indicate substantial damping of the precipitation signal, consistent with longer water residence times, greater mixing, and larger storage volumes. Conversely, values approaching 1 suggest minimal damping and rapid flow paths.

However, interpretation of ITTPs must also account for fractionation processes. In particular, evapotranspiration (ET) selectively removes lighter isotopes (^{16}O), enriching the remaining water in heavier isotopes (^{18}O). This enrichment can artificially increase the variance of $\delta^{18}\text{O}$ in near-surface or shallow soil water compartments, inflating ITTP values even in systems with relatively slow transit times (Tetzlaff et al., 2009). This is especially relevant in arid and semi-arid regions, where ET can dominate the water balance during dry seasons.

3.5 Hydraulic connectivity estimation

Structural Equation Modeling (SEM) has been widely applied in water science to evaluate complex relationships among hydrological, geological, and anthropogenic variables, particularly in studies of groundwater contamination and water quality degradation (Wu, 2010; Lupi et al., 2019; Xie et al., 2025). In this study, SEM is used explicitly as an exploratory, hypothesis-generating tool to assess potential hydrological connectivity among water sources based on dual-isotope ($\delta^2\text{H}$ – $\delta^{18}\text{O}$) data from rainfall, pond water, spring water, pore water, and fissure water. SEM is not a mass-conserving or process-based flow model, nor is it used here to infer volumetric fluxes, recharge rates, or source apportionment. Instead, it serves as a statistical consistency

check on hypothesized connectivity, identifying direct and indirect associations among water bodies that are evaluated in conjunction with tracer evidence and hydrometric observations.

Within the SEM framework, path relationships are primarily explained through two types of effects: The direct effect refers to the immediate impact of one variable on another through a single path, typically quantified as a standardized regression coefficient. Total effect represents the overall impact of one variable on another through all possible paths (including both direct and indirect), calculated as the sum of the direct effect and all indirect effects. Comparing direct and total effects allows identification of intermediary linkages and dominant association structures within the hypothesized connectivity network.

Given the potential for isotopic signatures to be altered by evaporation, mixing, or other non-conservative processes, results must be interpreted with caution. Pathways with p values > 0.05 were excluded during model refinement, and the final model met standard goodness-of-fit criteria (degrees of freedom < 3 , RMSEA < 0.05 , CFI > 0.95 , NFI > 0.95). SEM analysis was conducted using SPSS Amos 26.0 (IBM SPSS, Chicago, Illinois, USA).

In addition, we applied variance partitioning to evaluate the relative contributions of different water sources to pore and fissure water. This method decomposes the total variance in isotopic composition into components attributable to individual sources (e.g., precipitation, pond water, spring water), offering a complementary estimate of source influence. While useful, this approach remains subject to the same limitations as SEM, particularly the challenges of isotopic overlap and limited resolution in environments affected by mixing and evaporation (Lai et al., 2022).

To further constrain recharge pathways, we incorporated chloride ion (Cl^-) as a conservative tracer. Unlike stable isotopes, Cl^- behaves conservatively with respect to fractionation, and when interpreted alongside isotopes, it can further explain mixing and recharge pathways. Chloride concentrations in all water samples were analyzed using an ion chromatograph (DIONEX ICS-1100) at the College of Natural Resources and Environment, Northwest A&F University, China. Each sample was analyzed in triplicate, with charge balance errors maintained below 5 % to ensure analytical accuracy. This rigorous approach enhances the reliability of chloride data, supporting its integration with isotopic indicators in source attribution.

3.6 Groundwater recharge

Groundwater recharge in the gully zone is quantified using the water table fluctuation (WTF) method, which infers recharge and discharge events from temporal changes in groundwater levels (Healy and Cook, 2002; Gumuła-Kawecka et al., 2022). We recognize that recharge can originate from three hydrological sources: (1) surface water;

(2) the unsaturated zone (3) and the saturated zone (Scanlon et al., 2002; Wang et al., 2024). Among these, estimates based on the saturated zone are generally most reliable, as recharge from the unsaturated zone reflects potential inputs that may never reach the water table (Beven and Germann, 2013; Huang et al., 2019). The WTF method is widely used for estimating saturated zone recharge due to its high temporal resolution and conceptual simplicity (Xu et al., 2024). Based on previous site-specific studies (Wang et al., 2024), this method is well-suited for our analysis.

The water table fluctuation method assumes that changes in the groundwater table result solely from recharge or discharge, assuming a constant specific yield (S_y) over time (Healy and Cook, 2002; Obuobie et al., 2012). The formula is as follows:

$$R_i = S_y \frac{\Delta H_i}{\Delta t} \quad (4)$$

where, R is the groundwater recharge (mm), S_y is the specific yield of the aquifer, ΔH_i (where $\Delta H_i > 0$) is rise in groundwater level between days $i - 1$ and i , and Δt is the time interval (1 d). Specific yield, which represents effective drainable porosity of the shallow gully aquifer system, rather than soil water release from the unsaturated zone. In this study, S_y was estimated using two complementary approaches: (1) an empirical method based on soil texture to constrain plausible ranges of drainable porosity, and (2) the test pit method, in which S_y is calculated as the difference between total porosity and field water capacity (Liang et al., 2016). These approaches provide an estimate of aquifer-scale effective specific yield appropriate for shallow unconfined groundwater systems in loess-derived gully environments.

Empirical values for soil texture are referenced in Table A1. The test pit method for estimating S_y is described as follows:

$$S_y = TP - FWC \quad (5)$$

where, TP (total porosity) and FWC (field water capacity) were measured using the cutting ring method.

We applied two methods to calculate the daily groundwater table increments (ΔH_i). The RISE method assumes that recharge occurs only when the groundwater table elevation increases between two consecutive days (Gumuła-Kawęcka et al., 2022). Thus, $\Delta H_i = H_i - H_{i-1}$ if $H_i > H_{i-1}$, otherwise, $\Delta H_i = 0$. The master recession curve (MRC) method assumes that, in the absence of recharge, the groundwater table declines daily by a specific amount (ΔH_{MRCi}). This amount represents a simplified approximation of discharge processes in the aquifer, particularly lateral outflow to nearby surface water bodies. MRC establishes a functional relationship between a daily decrement of the water table (ΔH_{MRCi}) and the water table elevation (H_{i-1}) during periods without recharge.

$$\Delta H_{MRCi} = A \cdot H_{i-1} + B \quad (6)$$

where, the coefficients A and B were fitted for each piezometer based on data from periods of continuous groundwater table decreases lasting longer than two weeks. The daily water table increment due to recharge was then calculated as: $\Delta H_i = H_i - H_{i-1} + \Delta H_{MRCi}$ if $H_i > (H_{i-1} - \Delta H_{MRCi})$, otherwise, $\Delta H = 0$.

Notably, we used water dynamics from 24 October 2023, to 24 October 2024, to calculate pore water recharge, as this period exhibited clear groundwater fluctuations, making it more representative.

4 Results

4.1 Soil properties

The upper 50 cm of the soil profile is composed primarily of silt ($64.6 \pm 0.6\%$), with smaller but nearly equal proportions of clay ($18.0 \pm 1.3\%$) and sand ($17.4 \pm 1.6\%$), classifying the loess as silt loam according to the International Union of Soil Sciences (IUSS) scheme (Fig. 4a). Total porosity and field water capacity decreased slightly with depth, averaging $24.5 \pm 1.9\%$ and $21.3 \pm 1.7\%$, respectively (Fig. 4b). Specific yield remained relatively consistent within the 10–50 cm depth interval, averaging $3.2 \pm 0.8\%$, falling within the expected empirical range for silt loam soils (2%–7%) (Fig. 4c).

4.2 Hydrological signatures of rainfall, surface water, and groundwater sources

Pond water and rainfall exhibit similar spatial isotopic patterns, with more positive $\delta^2\text{H}$ values ($\delta^2\text{H} > -55\text{‰}$) than spring water, pore water, and fissure water (Fig. 5a, b). These values are line with the notion of direct rainfall and Hortonian runoff are the primary source of pond water. In contrast, the $\delta^2\text{H}$ values of pore, spring, and fissure water show little seasonal variation and are consistently more negative ($\delta^2\text{H} < -55\text{‰}$), than mean rainfall, indicating longer residence times and reduced evaporative influence.

The $\delta^2\text{H}$ – $\delta^{18}\text{O}$ relationships and box plots for each water source reveal key insights into the dominant hydrological processes occurring during the rainy season (Fig. 6). Firstly, rainfall follows a Local Meteoric Water Line (LMWL) of $\delta^2\text{H} = 7.7 \cdot \delta^{18}\text{O} + 8.9$ ($R^2 = 0.95$), which is closely aligned, though slightly offset, from the Global Meteoric Water Line (GMWL: $\delta^2\text{H} = 8 \cdot \delta^{18}\text{O} + 10$) (rainy season; Fig. 6a, c). This alignment indicates that precipitation in the region has a typical meteoric origin. Additionally, minimal evaporative enrichment occurred prior to collection. The relatively wide interquartile range of rainfall $\delta^{18}\text{O}$ values suggests that precipitation was derived from storm systems with considerable isotopic variability, reflecting differences in rainfall intensity, air mass origin, and temperature. However, this variability remains moderate compared with global patterns that span extreme rainfall events and broader climatic gradients.

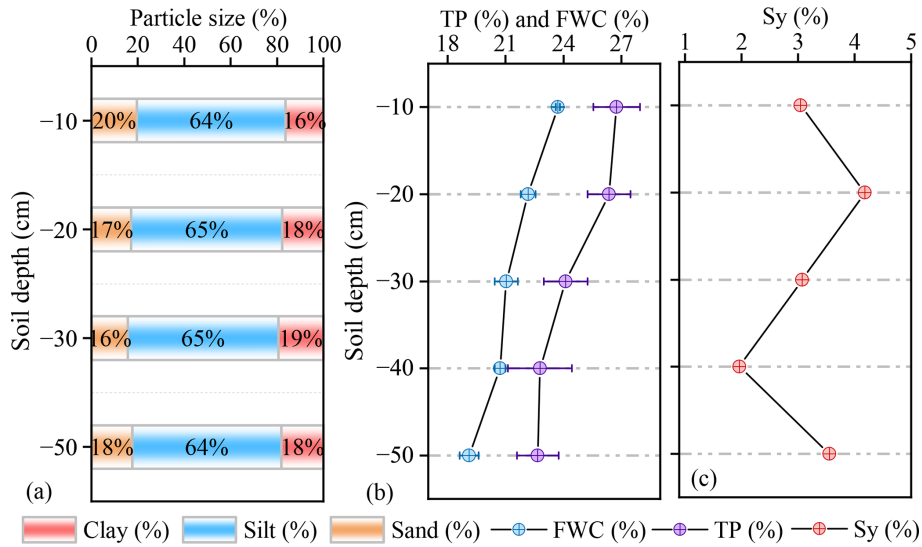


Figure 4. Vertical variation in soil texture and water retention characteristics in the gully region of the Loess Plateau. (a) Soil particle size distribution by depth, showing relatively uniform composition across layers (10–50 cm), dominated by silt (64%–65%), with moderate clay (16%–20%) and low sand (16%–20%) content. This fine-textured profile supports high moisture retention and slows infiltration, promoting delayed recharge. (b) Depth profiles of total porosity (TP) and field water capacity (FWC) reveal decreases with depth to 40 cm, with FWC reaching ~27%, suggesting greater water-holding capacity in subsoil layers and enhanced buffering of infiltrated water. (c) Vertical variations in the Specific Yield (S_y) across different soil layers. Collectively, these physical properties reflect a vertically stratified soil system where near-surface layers regulate infiltration pulses, and deeper layers act as long-term storage, shaping the timing and magnitude of subsurface recharge.

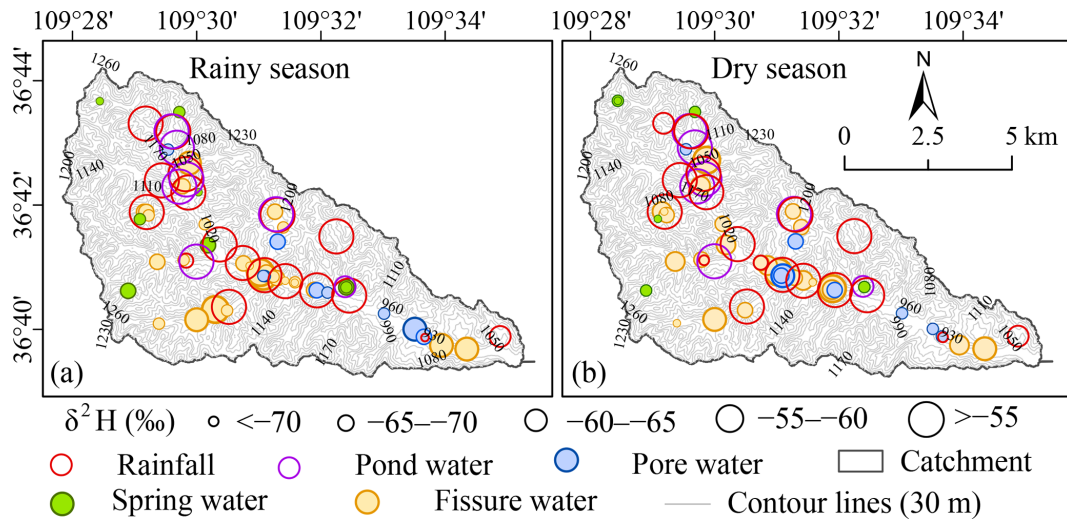


Figure 5. The spatial distributions of $\delta^2\text{H}$ values during the (a) rainy season and (b) dry season for rainfall, pond water, spring, pore water, and fissure water in the gully region of the Loess Plateau. To highlight spatial differences among water sources, $\delta^2\text{H}$ values were classified into five intervals: $< -70\text{‰}$, -70‰ to -65‰ , -65‰ to -60‰ , -60‰ to -55‰ , and $> -55\text{‰}$. Sampling points are color-coded by water type: red for rainfall, purple for pond water, blue for pore water, green for spring water, and orange for fissure water.

Pond water, in contrast, exhibits a clear evaporation signature with a shallower slope of $\delta^2\text{H} = 5.6 \cdot \delta^{18}\text{O} - 17.1$ (rainy season; $R^2 = 0.95$), $\delta^2\text{H} = 4.6 \cdot \delta^{18}\text{O} - 20.7$ (dry season; $R^2 = 0.74$). This signature aligns with expectations for surface water bodies, where open exposure facilitates fractionation. The box plot shows strong evaporative enrichment,

with median values shifted significantly toward more positive $\delta^{18}\text{O}$ and $\delta^2\text{H}$ compared to rainfall (Fig. 6a, c). Pond water maintains a relatively consistent slope and range across seasons, reinforcing its stable evaporative signature and less dynamic recharge behavior.

Spring water shows a clear seasonal transition in its isotopic composition. In the rainy season, its evaporation line ($\delta^2\text{H} = 6.2 \cdot \delta^{18}\text{O} - 11.4$; $R^2 = 0.75$) falls closer to the LMWL, suggesting that spring discharge is augmented by recent rainfall, likely delivered through rapid infiltration and shallow subsurface flow pathways during high-intensity events (Fig. 6a, b). However, the isotopic values of spring water are substantially more depleted than those of precipitation, indicating that older water stored in the porous subsurface aquifer dominates the overall spring flow composition composed of new and relatively old water.

During the dry season, the isotopic slope flattens and deviates further from the Local Meteoric Water Line (LMWL), reflecting increased evaporative influence or prolonged residence times (Fig. 6c, d). This seasonal shift suggests that as rainfall inputs decline, spring discharge becomes increasingly composed of slow-draining, older water that has undergone greater isotopic modification, either through mixing or evaporation in near-surface storage zones. Collectively, these patterns suggest that spring water acts as a dynamic integrator of recharge processes, rapidly responding to event-driven infiltration during the rainy season, yet also reflecting the delayed mobilization of older water stored in the subsurface. This behavior may be partly explained by a piston-like displacement mechanism, where incoming rainfall pushes pre-existing groundwater toward discharge zones.

Pore and fissure water show remarkably similar isotopic signatures during the rainy season. Pore water, again sampled from a porous subsurface aquifer, follows a fitted line of $\delta^2\text{H} = 4.3 \cdot \delta^{18}\text{O} - 27.9$ (rainy season; $R^2 = 0.74$), while fissure water, likely drawing from the same aquifer but through weathered bedrock pathways, fits $\delta^2\text{H} = 3.7 \cdot \delta^{18}\text{O} - 32.0$ (rainy season; $R^2 = 0.70$). These slopes are significantly flatter than those of rainfall, pond, or spring water, a pattern interpreted as evidence of evaporation prior to recharge or mixing with evaporated surface water. However, the box plots of the isotope data present a different picture. Both pore and fissure waters are systematically more depleted in $\delta^{18}\text{O}$ and $\delta^2\text{H}$ than precipitation, and their narrow interquartile ranges suggest a relatively uniform isotopic composition (Fig. 6a–d).

These depleted and uniform isotopic compositions indicate recharge dominated by isotopically light rainfall events, primarily intense summer monsoon storms, rather than evaporative enrichment. Depleted groundwater signatures thus reflect recharge from these summer events, with percolation delayed to cooler seasons due to soil storage and reduced evaporation. The flat regression slopes and narrow interquartile ranges are reconciled by longer residence times and mixing in the subsurface aquifer, which acts as a hydrological buffer that dampens seasonal isotopic variability (Table A2).

Complementing the isotope data, Cl^- levels in pore water consistently fall between those of precipitation and pond water across both seasons (Fig. 7a), and the correlation pattern between chloride concentration and $\delta^{18}\text{O}$ supports a mixed

recharge origin for pore water (Fig. 7b). This trend aligns with the isotopic evidence from the rainy season and supports the interpretation that pond water contributes to pore water recharge via vertical percolation through the vadose zone, particularly during high-rainfall periods when infiltration capacity is exceeded.

The inverse transit time proxies (ITTPs) broadly support the dual-isotope interpretations of water source dynamics. Pond water exhibited the highest ITTP values (1.5 ± 0.7), indicating rapid turnover and limited subsurface storage. These elevated values likely reflect inputs from direct rainfall and overland flow, as well as evaporative enrichment, which increases isotopic variability and can artificially shorten the apparent residence time. In contrast, pore water (0.7 ± 0.3) and fissure water (0.6 ± 0.5) showed lower ITTPs, consistent with longer residence times, greater subsurface mixing, and attenuation of seasonal isotopic signals due to delayed recharge. Spring water had the lowest ITTPs (0.3 ± 0.2), reflecting slow subsurface transport and integration of older water sources (Fig. 8).

4.3 Hydrological linkages and recharge efficiency

The SEM analysis reveals significant hydrological linkages among different water bodies in the catchment, with particularly well-defined pathways connecting rainfall, pond water, pore water, and fissure water (Fig. 9a, b). Rainfall contributes over 73 % to pore water recharge, far exceeding the < 17 % contribution from pond water (Fig. 9c). However, the SEM results indicate that the direct effect of pond water on pore water is stronger than that of rainfall (Fig. 9b). This apparent contradiction likely stems from the strong statistical association between rainfall and pond water, as pond water is primarily derived from rainfall and shares similar isotopic signatures.

These findings underscore the importance of integrating multiple lines of evidence rather than relying solely on SEM outputs. For example, chloride concentrations in pore water more closely resemble those of pond water, suggesting that pond water may contribute to pore water recharge under specific spatial or temporal conditions (Fig. 7a). The spatial distributions of chloride concentration and $\delta^{18}\text{O}$ further show that part of the pore water plots near the precipitation–pond water mixing line, providing evidence that pond water can contribute to pore water recharge, particularly in localized areas or during discrete recharge events (Fig. 7b). At deeper levels, the linkage between pore water and fissure water is supported by their nearly identical isotope values and similar ITTPs, suggesting a shared subsurface origin and a strong hydrological connection (Fig. 9a, b). In contrast, although there is some hydrological connectivity between pore water and spring water, differences in isotopic slopes and residence times may lead to an overestimation of their interaction. However, their nearly identical spatial distributions

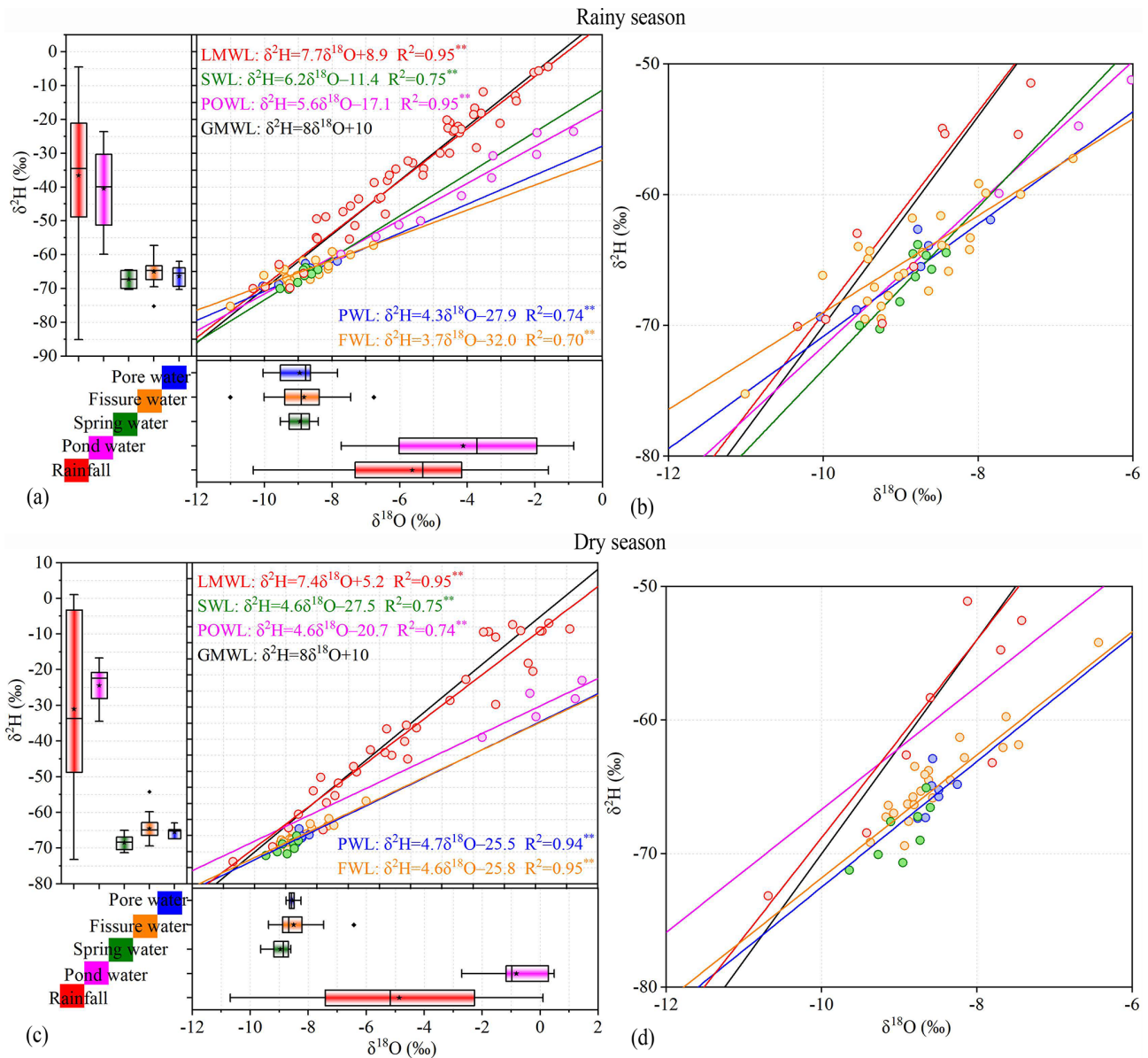


Figure 6. Dual stable isotopic compositions of rainfall, pond water, spring water, pore water, and fissure water during the rainy season and dry season in the gully region of the Loess Plateau. The black line represents the global meteoric water line (GMWL, $\delta^2\text{H}=10+8\delta^{18}\text{O}$). GMWL is the global meteoric water line of Craig, LMWL is the local meteoric water line, SWL is the spring water line, POWL is the pond water line, FWL is the fissure water line, and PWL is the pore water line. Panels (b) and (d) are magnified views of (a) and (c), respectively, highlighting the isotopic compositions of pore water, fissure water, and spring water (x axis: -12‰ to -6‰ ; y axis: -80‰ to -50‰).

of chloride concentrations and $\delta^{18}\text{O}$ provide more direct and reliable evidence of connectivity.

Although the model results initially suggest that rainfall, mediated through pond water, is the primary source of pore water recharge, discrepancies among the different indicators call for a more critical interpretation of the evidence. The contradictions observed across isotopic, chloride, and ITTP data underscore the need for further quantitative validation. To address the contradictions observed in the SEM and variance partitioning results, we apply the water table

fluctuation method to independently estimate the recharge rate from rainfall to pore water. Groundwater level fluctuations in the gully system revealed clear seasonal recharge dynamics, with an initial rise in the pore water table beginning on 24 October 2023, followed by a decline through early spring (1 March 2024) and a gradual recovery starting 20 June 2024 (Fig. 10a). Between 24 October 2023, and 24 October 2024, cumulative recharge was estimated at 238.0 ± 6.0 mm (RISE) and 241.4 ± 6.0 mm (MRC), with 159 and 167 recharge days, respectively (Fig. 10b, c). Given that

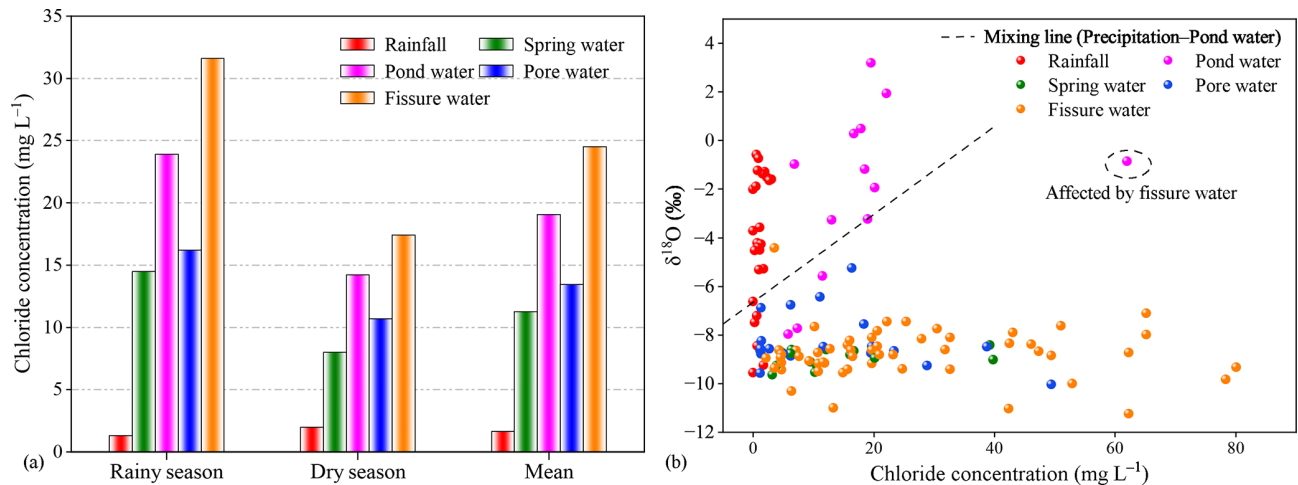


Figure 7. Chloride concentration of various water sources in the rainy and dry seasons (a), and the spatial relationship between chloride concentration and $\delta^{18}\text{O}$ for different water sources (b).

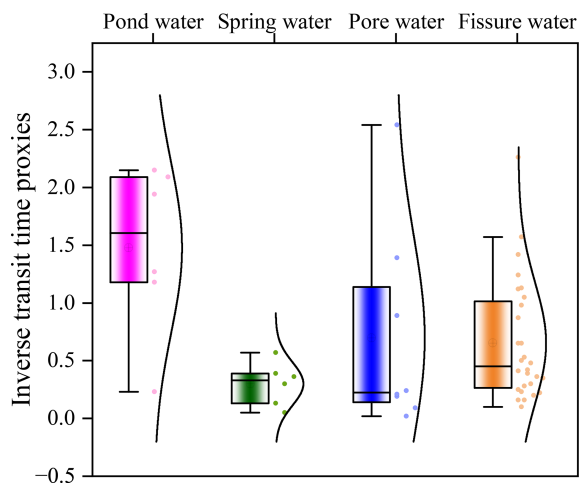


Figure 8. Boxplots and kernel density estimates of inverse transit time proxies (ITTPs) for pond water, spring water, pore water, and fissure water. Higher ITTP values indicate shorter water transit times since precipitation, while lower values suggest longer residence and greater isotopic damping. Pond water exhibited the highest and most consistent ITTPs (median ≈ 1.5), implying rapid recharge from recent rainfall or stormflow. Spring water showed the lowest ITTPs (≈ 0.3), consistent with longer subsurface flow paths and storage. Pore and fissure water displayed intermediate and more variable ITTPs, reflecting mixing between recent and older water sources, as well as seasonal differences in infiltration and soil moisture replenishment.

annual precipitation totaled approximately 550 mm, “site-scale” recharge was approximately 43%–44%, underscoring the significance of focused infiltration in sustaining shallow aquifer recharge within the gully environment.

Site-scale recharge is lower than the precipitation-to-pore water contribution estimated by the variance decomposition

method and may more accurately reflect “actual” recharge, as statistical estimates can be biased by similarities in isotopic signatures. Combined with dual-isotope and SEM analyses, the WTF results support a conceptual model where storm runoff is captured and redistributed through loess soils and retention structures, enabling both shallow and deeper subsurface flow. These flow paths link pore water, fissure water, and spring discharge across the complex gully landscape, reflecting both vertical and lateral connectivity within the groundwater system.

5 Discussion

5.1 Isotopic compositions of various water bodies in the gully region

In hydrological studies, the isotopic composition of water bodies reflects both sources and changes in hydrological processes (Wan and Liu, 2016; Kumar et al., 2019; Dasgupta et al., 2024). Precipitation, surface water, and groundwater usually exhibit differences in isotopic characteristics due to variations in evaporation, infiltration, and mixing (Gleeson et al., 2016; Kuang et al., 2019; Al-Oqaili et al., 2020). However, similar isotopic distributions among different water bodies often indicate a strong hydrological connection in their water sources (Yang and Wang, 2023).

Our study found that rainfall and pond water have similar spatial isotopic distribution patterns, indicating that pond water primarily originates from rainfall. This reflects the region’s geographical and hydrological characteristics. In this severely eroded gully region, the local government has constructed an extensive network of ponds and check dams to capture hillside runoff (Liu et al., 2017; Xue et al., 2025). As a result, most precipitation from the hills converges into these gully ponds and check dams. A lower pond water line

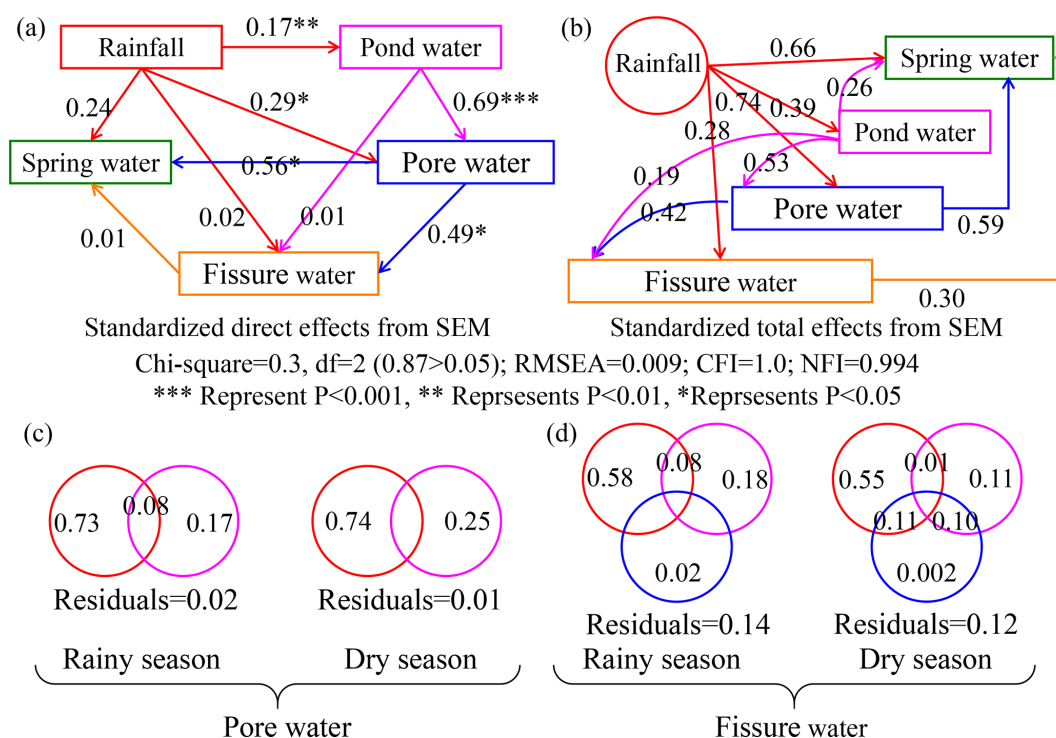


Figure 9. Structural equation modeling (SEM) and variance partitioning results illustrating hydraulic connectivity among water sources in the gully region of the Loess Plateau. Panels (a) and (b) show the standardized direct (a) and total effects (b) among rainfall, pond water, pore water, spring water, and fissure water, based on $\delta^{18}\text{O}$ and $\delta^2\text{H}$ data. In SEM, the total effect includes both direct pathways (a; e.g., rainfall \rightarrow pore water) and indirect pathways mediated by other variables (b; e.g., rainfall \rightarrow pond water \rightarrow pore water). Arrows indicate hypothesized water flow pathways, with line thickness proportional to effect size. Asterisks denote statistical significance ($* P < 0.05$, $** P < 0.01$, $*** P < 0.001$). The model fit is excellent ($\chi^2 = 0.3$, $df = 2$, $RMSEA = 0.009$, $CFI = 1.0$, $NFI = 0.994$), supporting the robustness of these inferred connections. Panels (c) and (d) present variance partitioning results showing the relative contributions of source waters to pore water and fissure water during the rainy and dry seasons, respectively. In panel (c), rainfall (red) and pond water (pink) explain a large portion of pore water variability, with some shared explanatory power and modest residuals. In panel (d), fissure water reflects a more complex origin, with contributions from rainfall (red), pond water (pink), and pore water (blue), and greater overlap and residuals, especially during the dry season.

slope indicates evaporation fractionation during retention. Evaporation preferentially removes lighter isotopes (^1H and ^{16}O), enriching heavier isotopes (^2H and ^{18}O) and shifting the pond water's isotopic composition from its precipitation source (Araguás-Araguás et al., 1998; Zhang and Wu, 2009; Gleeson et al., 2016). This similarity is primarily due to the fact that pond water originates from rainfall and its runoff in the hilly-gully region (Liu et al., 2011; Ji et al., 2024). Additionally, the isotopic values of most groundwater in the gully areas are more depleted compared to those of rainfall and pond water, likely due to the recharge mechanisms and residence times of different groundwater types, and the inherent isotopic characteristics of their primary recharge sources (El Ouali et al., 2024). The depleted signatures in groundwater reflect preferential capture of isotopically light summer monsoon events, with effective percolation delayed to cooler seasons due to transient soil storage and minimized evaporation, consistent with observed water table rises predominantly from October to April. Nevertheless, these values fall

within the range of precipitation isotopic values, leaning towards the more negative end. This suggests two complementary mechanisms: (1) the thin unsaturated zone ($< 10\text{ m}$) provides preferential pathways for rapid infiltration of precipitation, minimizing evaporative fractionation, and (2) groundwater is likely recharged primarily by intense precipitation events (e.g., summer storms) with inherently more negative isotopic signatures (Liu, 2024). Together, these processes explain the observed isotopic characteristics of groundwater.

To further investigate the complexity of different types of groundwater in the gully area, we conducted hydrological and geological surveys, collecting water samples from spring water, pore water, and fissure water. The results show that the isotopic values of spring water, pore water, and fissure water are closely clustered, indicating a strong interconnection among the different types of groundwater within the hydrological cycle. This is likely due to their shared geological and hydrological environments (Bouwer, 2002; Li et al., 2021; Zhang et al., 2023). Our study found that the water

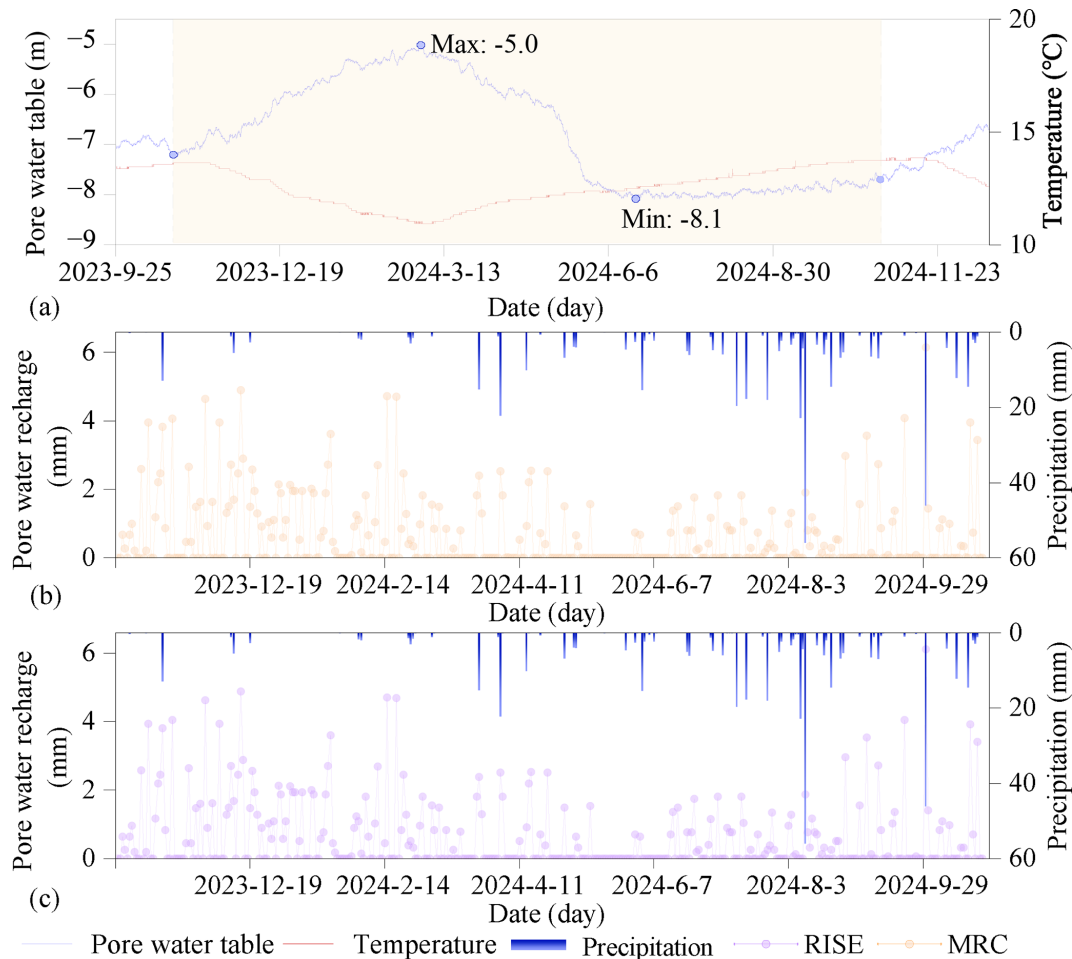


Figure 10. Temporal dynamics of pore water table depth, temperature, precipitation, and recharge in the gully region of the Loess Plateau. (a) Daily time series of pore water table depth (blue line) and surface temperature (red line) from September 2023 to November 2024. The water table fluctuates seasonally, rising from ~ -8.1 m in late summer to a maximum of ~ -5.0 m in early spring (March 2024), indicating delayed infiltration and cool-season recharge. (b) Daily precipitation (blue bars) and modeled pore water recharge estimates using the MRC methods. (c) Daily precipitation (blue bars) and modeled pore water recharge estimates using the RISE methods. Most recharge events occur from October to April, even when rainfall is not especially high, while warm-season precipitation contributes little to recharge, likely due to increased evaporative losses and shallow soil retention. Together, these patterns suggest strong seasonal control on recharge processes, with effective infiltration primarily occurring during cooler, low-evaporation periods.

line slope of pore water and fissure water was higher in the dry season than in the rainy season, with values falling between the slopes of pond water from the rainy and dry seasons. To investigate the cause of these results, we analyzed groundwater level dynamics, which showed that water tables were lower at the end of the rainy season but rebounded afterward, making dry-season tables higher. This suggests that rainy-season groundwater mixes with evaporatively enriched water, lowering its slope, while dry-season groundwater is recharged by delayed rainfall and pond water, increasing its slope. These findings reveal that isotopic composition is influenced by both current and prior hydrological conditions. They also highlight the complexity of evaporation fractionation regulated by water mixing and demonstrate the signif-

icant impact of pond construction on groundwater recharge and regional hydrology in the gully regions.

5.2 Groundwater recharge processes in the gully region

In recent years, discussions of groundwater recharge sources on the Loess Plateau have largely focused on tableland and hilly areas characterized by thick loess deposits, whereas gully regions have received comparatively limited attention (Li et al., 2017; Xiang, 2021; Lu, 2020). For instance, Liu et al. (2011) demonstrated that groundwater near valley bottoms in hilly loess areas can be replenished by a combination of precipitation, runoff, and surface water. Our results are broadly consistent with these earlier findings, but extend them by providing multiple lines of site-specific evi-

dence. Based on stable isotope signatures and chloride concentrations, we independently identify precipitation and surface water as the primary sources of groundwater recharge in gully systems. Furthermore, by applying a structural equation model (SEM), we quantitatively evaluate the relative importance of different recharge pathways, demonstrating that surface water (particularly pond water) plays a key mediating role in transferring precipitation inputs to subsurface pore water. Building on these results, we classify groundwater in the study area into three functional types, spring water, pore water, and fissure water, and propose a progressive, multi-stage recharge framework: (1) direct recharge of pond water by precipitation and indirect recharge of pore water by precipitation; (2) focused recharge from pond water to pore water; and (3) downward percolation from pore water to fissure water. This framework highlights the complexity of groundwater flow and recharge processes in gully-dominated landscapes and underscores the significant influence of human interventions, such as ponds and check dams, on modifying hydrological connectivity and recharge dynamics.

In the deep-profile unsaturated zones of the hilly region on the Loess Plateau, previous studies have used chloride mass balance and tritium peak methods to estimate groundwater recharge from precipitation, typically accounting for 2%–22% of annual rainfall, with water residence times in the unsaturated zone lasting several years or even hundreds of years (Huang and Pang, 2011; Tan et al., 2016; Li et al., 2017; Wang et al., 2024). However, these studies did not address the catchment role of gully regions. Field observations and past studies show that precipitation rarely directly infiltrates thick loess in hilly areas (Xu et al., 1993; Li, 2001). Instead, it forms surface runoff that converges into engineered gullies and accumulates in ponds or other water bodies (perched water), serving as a concentrated recharge source for groundwater (Yu et al., 2025), reflecting the sustained and delayed impact of gully runoff on groundwater recharge, which is consistent with the results of this study. In summary, while hillslope-scale studies describe a “dispersed recharge” mode, where precipitation percolates slowly through thick unsaturated zones, this study identifies a “concentrated recharge” mode in engineered gullies, driven by runoff convergence and regulated by check dams via ponding. These fundamentally distinct modes, differing in hydrological processes, spatial scales, and recharge efficiencies, collectively enhance the understanding of groundwater recharge mechanisms on the Loess Plateau.

Notably, our study does not consider confined water. Tan et al. (2016) indicated that the groundwater in the high mountain-hilly loess aquifer does not originate from the upwelling of ancient regional groundwater, and there is no evidence of deep confined water beneath the loess strata in the high mountain-hills. Additionally, our findings represent only the groundwater recharge results in the gully regions for two reasons: (1) The hydrological system is complex, with significant variations across different landscapes of the Loess

Plateau (Li et al., 2019, 2021). For example, Li et al. (2019) found that groundwater dominates the hydrological system in the tableland on the Loess Plateau, where surface water (streams) is recharged by groundwater because river channels are deeper than the bedrock. (2) Our data collection focused on gully because the “Loess Liang” and “Loess Mao” hillside areas are covered by thick loess with minimal water sources.

5.3 Groundwater recharge rates in the gully region

In many parts of the world, identifying the sources of groundwater recharge and its renewability is essential for effective water resource management (Ajjur and Baalousha, 2021; Meles et al., 2024). In the hilly-gully region of the Loess Plateau, where groundwater is considered a crucial source of safe water, understanding the origins and recharge of aquifers provides valuable information for water resource planners (Wang et al., 2006; Liu et al., 2011; Wang et al., 2024). This knowledge is essential and should be shared with regions facing similar challenges.

Groundwater recharge can be quantified from three hydrological sources: surface water, the unsaturated zone, and the saturated zone (Scanlon et al., 2002). Recharge estimates based on the saturated zone are generally more reliable than those from the unsaturated zone, as the latter represents potential recharge that may not ultimately reach the groundwater table (Beven and Germann, 2013; Huang and Shao, 2019). The groundwater table fluctuation method is widely used for estimating saturated zone recharge due to its high temporal resolution and intuitive nature (Gumuła-Kawęcka et al., 2022; Xu et al., 2024). In our study area, ITTPs estimated similar transit times for both pore water and fissure water. Therefore, we used the groundwater table fluctuation method to assess the recharge of pore water in the gully region. The total recharge from 2023 to 2024 was estimated at 241.4 ± 6.0 and 238 ± 6.0 mm using the MRC and RISE methods, respectively. Under constant specific yield conditions, the MRC method typically estimates higher groundwater recharge and recharge days than RISE, as it accounts for groundwater table decline due to lateral outflow and other discharge processes in the absence of recharge (Hepner and Nimmo, 2005). Our findings support this pattern. Furthermore, the key parameter for estimating groundwater recharge using the water table fluctuation method is specific yield (S_y), which depends on soil properties and water table depth (Liang et al., 2015). Shallow soil measurements (0–50 cm) using the test pit method (total porosity minus field capacity) yielded $S_y \approx 0.03$, consistent with high capillary retention in near-surface loess (Wang et al., 2024). However, for water tables deeper than 2 m (as in this study, typically 4–10 m), the test pit method provides a reliable estimate of aquifer-scale drainable porosity (Nachabe, 2002; Shah and Ross, 2009; Liang et al., 2015). Accordingly, we adopted $S_y = 0.032$, aligned with values of ~ 0.03 reported

for similar loess-derived unconfined aquifers on the Loess Plateau (Wang et al., 2023). Sensitivity analysis indicates that recharge estimates vary by approximately $\pm 25\%$ across the plausible S_y range (0.032 ± 0.008), reflecting uncertainty in effective drainable porosity within shallow gully aquifers.

Research on groundwater recharge in the Loess Plateau has mainly focused on deep-profile unsaturated zones in the tableland and hilly areas, with tracer methods estimating recharge between 9 to 100 mm (Huang and Pang, 2011; Li et al., 2017; Xiang et al., 2019; Lu, 2020; Wang et al., 2024). In contrast, our study in the gully region indicates recharge of up to 240 mm, much higher than previous estimates on deep-profile unsaturated zones. This difference reflects several factors: (1) Unsaturated zone thickness: In the gully region, the unsaturated zone is generally less than 10 m thick, much shallower than in tableland and hilly areas (mean thickness of 92.2 m), making infiltration easier and promoting effective recharge. (2) Gully topography and hydrology, characterized by well-developed channels, concentrated runoff, and widespread ponds and check dams, promote focused infiltration (Liu et al., 2017; Li et al., 2021; Xue et al., 2025). (3) Research methods: Tracer methods reflect long-term recharge rates and are better suited for thicker unsaturated zones (Huang and Pang, 2011; Lu, 2020; Li et al., 2017). In contrast, the water table fluctuation method directly captures short-term recharge dynamics and works better in thinner unsaturated zones. Moreover, this method also better captures surface water-groundwater interactions and focused recharge effects (Gumuła-Kawęcka et al., 2022). These findings underscore the importance of studying recharge in gully regions, filling a research gap in the Loess Plateau's geomorphology and providing new ecohydrological insights. However, the robustness of our findings requires further exploration. On one hand, due to the limited spatial distribution of sampling points, the current results primarily reflect the hydrological characteristics of engineered gullies, and their representativeness at the regional scale requires validation through future expansion of the monitoring network. On the other hand, the study period did not encompass extreme precipitation or drought events, which may significantly alter surface flow convergence conditions and vadose zone water transport mechanisms, thereby substantially impacting recharge processes. Future work should strengthen dynamic monitoring and simulation analysis under extreme hydrological scenarios.

5.4 Revised conceptual model

To convey our evolving understanding of the spatial structure and dynamics in the Gully Region, we developed a conceptual model that traces precipitation's transformation into subsurface water, from runoff capture and surface ponding in dammed gully reaches, through infiltration in the unsaturated zone, to recharge in both shallow porous aquifer and deeper bedrock fissure systems (Fig. 11). This conceptual re-

framing is grounded in the stark contrasts between hydrological processes active on hilly uplands and managed gully systems. In the hilly uplands, previous studies have shown that thick loess deposits, often exceeding 90 m (including low-permeability aquifers), combined with steep slopes ($> 15^\circ$) severely restrict vertical infiltration (Zhu et al., 2018; Huang et al., 2019; Huang et al., 2024). Compounded by short-duration, high-intensity rainfall events that provide insufficient moisture for deep profile wetting, rainfall is converted rapidly into surface runoff (Li et al., 2021). Our new work shows that runoff is systematically funneled downslope into gully systems as a consequence of ecological engineered check dams and retention ponds that intercept and concentrate overland flow. Most infiltration occurs after surface water accumulates in fill zones of engineered gullies. Ponds and perched water bodies subsequently serve as localized recharge foci.

Crucially, gully systems possess distinct hydrogeological characteristics: the loess mantle is much thinner (typically < 25 m), and the soils are dominated by silt loam textures with moderate specific yield (0.02–0.05) and high field capacity (21%–28%). These properties promote transient water storage and enable temporally delayed and depth-partitioned infiltration. Based on our integrated analyses of stable isotopes, chloride concentrations, and inverse transit time proxies, we find that engineered gullies function not as passive erosional features but as active, managed recharge conduits. This conceptualization captures a critical spatial transition, from runoff generation in the hilly uplands to focused recharge in gully zones, emphasizing the pivotal role of gully systems in regulating groundwater recharge across the Loess Plateau landscape.

Combined hydrological monitoring and multi-indicator analysis further reveal that following the rainy season, infiltration depths on hilly slopes are typically shallow (less than 1 m), while groundwater levels in gully areas exhibit pronounced rises exceeding 2 m (Fig. 11). Recharge estimates based on the water table fluctuations reach up to approximately 240 mm at the monitored gully reach, far surpassing values observed in deep unsaturated zones of tablelands and hills (Huang and Pang, 2011; Li et al., 2017; Lu, 2020; Wang et al., 2024). The results of this study reinforce the role of engineered gully reaches as focal points for groundwater recharge and further quantify site-scale pore-water recharge equivalent to $\sim 43\%$ of mean annual precipitation, a finding that highlights the efficiency of focused infiltration under managed conditions. This value reflects spatially focused recharge under conditions of runoff convergence and ponding, and should not be interpreted as representative of hillslope or catchment-wide recharge rates.

Liu et al. (2011) found that groundwater near valleys in the hilly loess area is replenished by precipitation, runoff, and surface water. Moreover, fissure water exhibits more depleted isotopic signatures and higher chloride concentrations, indicating deeper percolation of pore water or mix-

ing with older recharge sources (Fig. 11). These patterns, supported by ITTPs and statistical (SEM-based) connectivity indicators, reveal a hierarchical recharge sequence: event-driven infiltration enters a porous shallow aquifer, some of which slowly percolates into deeper fissure zones. This hierarchical mechanism is facilitated by the combination of thin loess mantles, engineered interventions (e.g., check dams and ponds), and delayed hydrological responses.

By integrating multiple lines of evidence, this conceptual model redefines engineered gullies as selective recharge corridors whose hydrological function emerges from the interaction between geomorphic structure and human intervention. It challenges the traditional view of gullies as purely erosional landforms and emphasizes their dual hydrological function: acting both as runoff conveyance channels and as transient reservoirs that store and redistribute water across space and time. This recharge capacity is jointly governed by topographic convergence, reduced loess thickness, and the presence of engineered structures such as check dams and retention ponds that increase residence time.

Crucially, the model offers insight into the multifunctionality of ecological engineering, particularly check dams and ponds, in enhancing groundwater recharge, and supporting ecosystem restoration across the Loess Plateau. This study proposes a cascade-type recharge framework for engineered gully systems, highlighting the role of engineered gullies as convergence pathways that locally focus infiltration and groundwater recharge. Rather than invoking preferential flow within the soil matrix, this framework emphasizes topographic convergence, stratigraphic thinning, and engineered ponding as the dominant mechanisms that promote spatially concentrated recharge within gully zones. While this process is demonstrated using site-specific tracer and water-table observations, its broader relevance at the catchment scale remains conceptual and warrants further investigation. Furthermore, water movement within the silted loess layer of the gully system remains dominated by a piston flow pattern (Yu et al., 2025). By identifying the pivotal role of gully systems in stormwater detention, delayed infiltration, and depth-partitioned recharge, this study establishes a mechanistically grounded conceptual basis improving water resource allocation, infrastructure planning, and groundwater sustainability in arid and semi-arid regions.

However, with the reconstruction of gully systems and ecological restoration, attention must also be given to the potential risks of pollutant migration (Yu et al., 2020). The hydrological functions of gullies may enhance the movement of pollutants into groundwater, especially in areas with intensive human activities, where pollutants can enter engineered gullies through surface runoff and subsequently infiltrate the groundwater system. During ecological restoration, excessive human intervention or soil improvement measures may lead to the accumulation and dispersion of pollutants, which may compromise groundwater security (Liu et al., 2017). Therefore, the protection and rational recon-

struction of gully systems should not only focus on their hydrological functions but also consider potential environmental risks, particularly the pathways of pollutant migration. These findings therefore underscore the need to evaluate gully-based restoration strategies within an integrated water-quality and groundwater-protection framework (Obuobie et al., 2012; Zhao et al., 2019; Zhao and Wang, 2021; Xue et al., 2025).

The study demonstrates how hydrologically arrested gully systems can function as critical “recharge windows” for groundwater in arid areas. This underscores the importance of strategically identifying and managing gully networks in watershed management, while avoiding excessive filling or hardening to preserve their hydrological functions. In ecological restoration projects, directing surface runoff toward engineered gullies under controlled conditions can efficiently convert limited precipitation into groundwater storage, thereby enhancing regional water retention capacity. Beyond advancing theoretical understanding of regional hydrological processes, this conceptual model provides a process-based foundation for developing spatially targeted models of groundwater recharge in managed dryland landscapes.

5.5 Limitations and future research directions

This study underscores the limitations of relying on a single indicator to infer localized groundwater recharge pathways, as doing so may lead to oversimplified or potentially misleading interpretations of complex hydrological processes. While stable isotope signatures suggest precipitation contributes to pore aquifer recharge, they do not provide clear evidence of direct recharge from pond water to either pore or fissure groundwater during the dry season. In contrast, the spatial distribution of chloride concentrations offers compelling support for focused pond water leakage into the shallow groundwater system.

Without explicit mass-balance constraints, structural equation modeling may not independently or quantitatively represent actual groundwater flow processes. In contrast, the water-table fluctuation method, which directly measures changes in groundwater levels, provides a more empirically grounded estimate of total recharge. Each approach nevertheless offers distinct strengths: water-table fluctuations resolve the timing and magnitude of recharge, whereas isotopic, hydrochemical, and modeling analyses yield critical insights into recharge sources and flow pathways. By leveraging the complementarity and mutual corroboration of these methods, our study robustly demonstrates the pivotal role of gully areas in groundwater recharge.

Despite effort to address uncertainties, limitations remain in terms of spatial and temporal sampling density. For example, the lack of long-term tracers such as groundwater age, combined with limited observations of groundwater level fluctuations, constrains our ability to assess recharge dynamics over multi-year timescales. Additionally, the current sam-

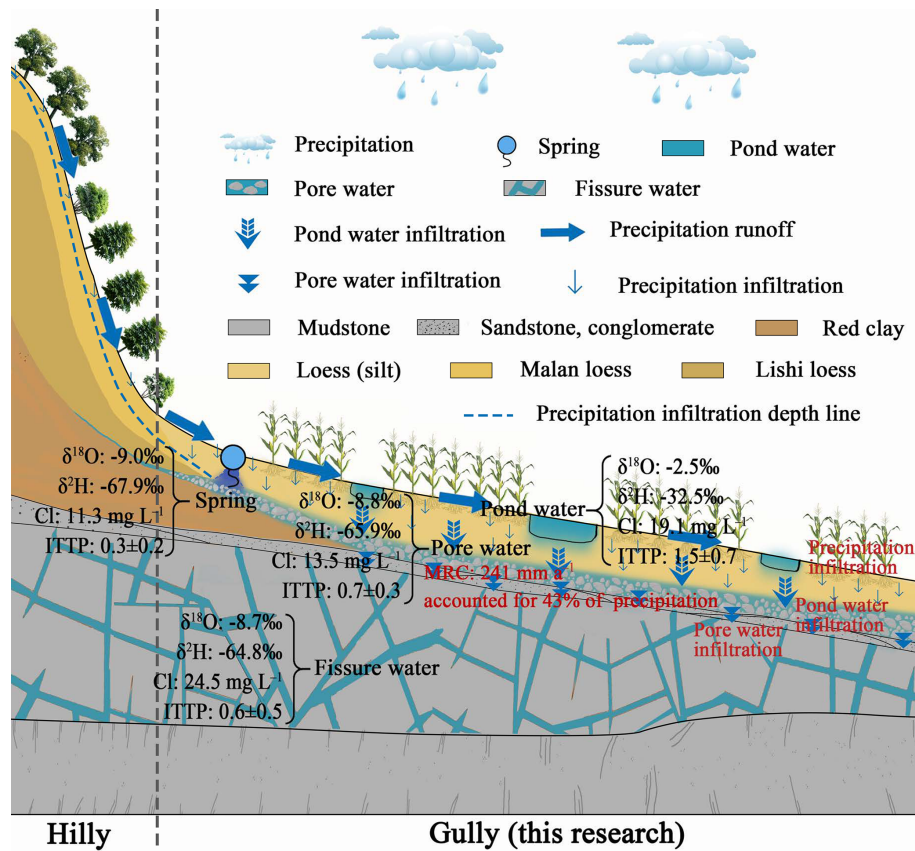


Figure 11. Hydraulic connections between different water bodies in the hilly-gully region of the Loess Plateau. The study area consists of hilly and gully regions. In the hilly area, the stratigraphic sequence from top to bottom is Malan loess, Lishi loess, red clay, sandstone, and mudstone. Rainfall infiltration within the Malan loess is less than 1 m, and the area is mainly covered by vegetation. In the gully area, the stratigraphy from top to bottom includes loess (silt), sandstone and conglomerate, and mudstone. Pore water is found within the sandstone and conglomerate, while fissure water occurs in bedrock fractures (mudstone). Numerous check dams or ponds are distributed throughout the gully area. The vertical separation between the pore water and pond water ranges from 3 to 5 m. Corn is the main crop cultivated in this region. Most springs in the study area are located at the junction of the hilly and gully regions and are discharged from pore water.

pling design includes only two campaigns during the rainy and dry seasons, which may be insufficient to fully capture the seasonal variability of ITTP values. This, in turn, may affect the accuracy of groundwater renewal frequency estimates and the strength of inferred hydrological connections. In arid and semi-arid regions, groundwater recharge is typically triggered by infrequent, high-intensity rainfall events. However, existing sampling strategies based on seasonal intervals often lack the temporal resolution necessary to capture these short-lived, event-driven recharge processes effectively.

Future research should address these issues through several improvements: (1) conducting higher-frequency, event-scale sampling to systematically monitor rainfall, spring discharge, and pond water level dynamics, thus capturing the influence of key hydrological events on recharge processes; (2) expanding the spatial coverage of pore and fissure well monitoring to improve the accuracy of regional recharge pattern identification; and (3) incorporating additional environ-

mental tracers (e.g., ^3H , ^{22}Na) to trace flow paths and estimate recharge lag times. In addition, systematic observation of event-scale hydrological processes should be strengthened by establishing a high-frequency, event-driven monitoring network to better capture the nonlinear coupling among rainfall, surface runoff, and groundwater dynamics. This approach would significantly improve our understanding of rapid infiltration events and associated recharge mechanisms.

From a methodological perspective, integrating statistical techniques, such as SEM and variance decomposition analysis, with process-based physical models like MODFLOW and HYDRUS can provide mechanistically constrained insights into recharge pathways. Compared to correlation-based statistical methods, physical models offer greater precision in characterizing groundwater flow and recharge processes across both temporal and spatial dimensions, helping to reduce uncertainties associated with non-conservative tracer behavior and the absence of mass balance constraints. Regarding measurements, hydrometric instrumenta-

tion within check dams and beneath pond beds could further quantify the recharge effects of various engineering interventions under specific hydrological conditions. Additionally, integrating isotopic data with mean transit time modeling, combined with targeted catchment-wide field monitoring and improved spatial analysis, could help elucidate recharge pathways, quantify temporal dynamics, and enhance process-level understanding of groundwater recharge throughout the catchment of such complex dryland landscapes. Collectively, these efforts will contribute to a stronger theoretical foundation and offer practical guidance for the precise management of water resources, the design of ecologically appropriate engineering interventions, and the implementation of effective landscape rehabilitation strategies.

6 Conclusion

Through integrated analysis of stable isotopes, chloride concentrations, water-table fluctuations, and inverse transit time proxies, this study provides multiple, convergent lines of evidence that engineered gully reaches on the Loess Plateau function as hydrologically significant recharge zones, rather than solely as products of accelerated erosion and degradation. Precipitation-driven runoff supports substantial recharge to shallow pore aquifers, with site-scale recharge magnitudes equivalent to approximately 43 % of mean annual precipitation at the monitored gully reach. Although evaporative fractionation limits the ability of stable isotopes alone to resolve direct recharge from ponded surface water, chloride concentrations provide independent evidence consistent with mixing between pond water and pore water, complementing the isotopic patterns. Together, these indicators indicate likely hydraulic connectivity, while not constituting a mass-balanced quantification of recharge sources. Recharge within shallow gully-zone aquifers is spatially concentrated and temporally selective, governed by topographic convergence, loess stratigraphy, and ecological engineering structures, particularly check dams and ponds, which increase surface-water residence time and promote focused infiltration.

These findings offer a process-based framework for developing hydrological indicators of landscape function and restoration performance managed in dryland environments. Specifically, recharge magnitude, isotopic damping, and solute accumulation patterns may serve as diagnostic indicators for identifying effective recharge zones and tracking hydrological response to intervention. To refine these indicators, future studies should incorporate high-frequency monitoring, event-based sampling, and multi-tracer approaches. Collectively, this work challenges conventional views of gullies as hydrological liabilities and demonstrates context-dependent role as targeted recharge assets in engineered dryland systems, refining conceptual understanding of dryland groundwater recharge and informing the evaluation and design of ecological engineering strategies in similar semi-arid landscapes.

Appendix A

Table A1. The specific yield of different texture of soil (adapted from Liang et al., 2016).

Texture	Average Specific Yield	Minimum Specific Yield	Maximum Specific Yield	Coefficient of Variation (%)
Clay	0.02	0.00	0.05	59
Silt	0.08	0.03	0.19	60
Sandy Clay	0.07	0.03	0.12	44
Fine Sand	0.21	0.10	0.28	32
Medium Sand	0.26	0.15	0.32	18
Coarse Sand	0.27	0.20	0.35	18
Gravelly Sand	0.25	0.20	0.35	21
Fine Gravel	0.25	0.21	0.35	18
Medium Gravel	0.23	0.13	0.26	14
Coarse Gravel	0.22	0.12	0.26	20

Table A2. Isotopic composition ($\delta^2\text{H}$ and $\delta^{18}\text{O}$) of various water sources in the rainy and dry seasons.

	Rainy season		Dry season	
	$\delta^2\text{H}$	$\delta^{18}\text{O}$	$\delta^2\text{H}$	$\delta^{18}\text{O}$
Rainfall	$-36.6 \pm 20.4\text{‰}$	$-5.6 \pm 2.3\text{‰}$	$-31.0 \pm 23.2\text{‰}$	$-4.9 \pm 3.0\text{‰}$
Pond water	$-40.5 \pm 13.1\text{‰}$	$-4.1 \pm 2.3\text{‰}$	$-24.5 \pm 6.9\text{‰}$	$-0.8 \pm 1.3\text{‰}$
Spring water	$-67.3 \pm 2.6\text{‰}$	$-9.0 \pm 0.4\text{‰}$	$-68.4 \pm 2.2\text{‰}$	$-9.0 \pm 0.4\text{‰}$
Pore water	$-66.3 \pm 3.1\text{‰}$	$-9.0 \pm 0.6\text{‰}$	$-65.4 \pm 3.8\text{‰}$	$-8.5 \pm 0.6\text{‰}$
Fissure water	$-65.0 \pm 3.8\text{‰}$	$-8.8 \pm 0.9\text{‰}$	$-64.5 \pm 5.5\text{‰}$	$-8.5 \pm 0.9\text{‰}$

Data availability. All datasets are available at Zenodo: <https://doi.org/10.5281/zenodo.18596600> (Ji et al., 2026).

Author contributions. ZXJ: Conceptualization, Methodology, Formal analysis, Investigation, Visualization, Data curation, Validation, Writing-original draft. ADZ: Conceptualization, Formal analysis, Validation, Visualization, Writing-review & editing. LW: Conceptualization, Funding acquisition, Project administration, Resources, Supervision, Visualization, Writing-review & editing.

Competing interests. The contact author has declared that none of the authors has any competing interests.

Disclaimer. Publisher's note: Copernicus Publications remains neutral with regard to jurisdictional claims made in the text, published maps, institutional affiliations, or any other geographical representation in this paper. The authors bear the ultimate responsibility for providing appropriate place names. Views expressed in the text are those of the authors and do not necessarily reflect the views of the publisher.

Acknowledgements. We gratefully acknowledge the Shaanxi Yan'an Forest Ecosystem Observation and Research Station (Beijing 100085, China) for their assistance during the fieldwork.

Financial support. This research has been supported by the National Natural Science Foundation of China, Key Programme (grant nos. 42377318 and U24A20629).

Review statement. This paper was edited by Philippe Ackerer and reviewed by two anonymous referees.

References

- Ajjur, S. B. and Baalousha, H. M.: A review on implementing managed aquifer recharge in the Middle East and North Africa region: methods, progress and challenges, *Water Int.*, 46, 578–604, <https://doi.org/10.1080/02508060.2021.1889192>, 2021.
- Al-Oqaili, F., Good, S. P., Peters, R. T., Finkenbiner, C., and Sarwar, A.: Using stable water isotopes to assess the influence of irrigation structural configurations on evaporation losses in semi-

- arid agricultural systems, *Agric. For. Meteorol.*, 291, 108083, <https://doi.org/10.1016/j.agrformet.2020.108083>, 2020.
- Araguás-Araguás, L., Froehlich, K., and Rozanski, K.: Stable isotope composition of precipitation over south-east Asia, *J. Geophys. Res.*, 103, 28721–28742, <https://doi.org/10.1029/98JD02582>, 1998.
- Berg, A., Findell, K., Lintner, B., Giannini, A., Seneviratne, S. I., Van den Hurk, B., Lorenz, R., Pitman, A., Hagemann, S., Meier, A., Cheruy, F., Ducharne, A., Malyshev, S., and Milly, P. C. D.: Land-atmosphere feedbacks amplify aridity increase over land under global warming, *Nat. Clim. Change*, 6, 869–874, <https://doi.org/10.1038/nclimate3029>, 2016.
- Beven, K. and Germann, P.: Macropores and water flow in soils revisited, *Water Resour. Res.*, 49, 3071–3092, <https://doi.org/10.1002/wrcr.20156>, 2013.
- Bouwer, H.: Artificial recharge of groundwater: hydrogeology and engineering, *Hydrogeol. J.*, 10, 121–142, <https://doi.org/10.1007/s10040-001-0182-4>, 2002.
- Cai, H. E., Zhang, J. W., Zheng, J. G., Zhang, R. S., and Liang, X. L.: Hydrogeology features of Loess hilly gully region in Yan'an, *Geotech. Eng. Tech.*, 33, 288–292, <https://doi.org/10.3969/j.issn.1007-2993.2019.05.009>, 2019.
- Dasgupta, B., Prakash, P., Sen, R., Noble, J., Chatterjee, S., and Sanyal, P.: The isotopic composition of the world's highest river basins: Role of hydrological mixing ratios and transit time, *J. Hydrol.*, 638, 131544, <https://doi.org/10.1016/j.jhydrol.2024.131544>, 2024.
- De Vries, J. J. and Simmers, I.: Groundwater recharge: an overview of processes and challenges, *Hydrogeol. J.*, 10, 5–17, <https://doi.org/10.1007/s10040-001-0171-7>, 2002.
- El Ouali, A., Roubil, A., Lahrach, A., El Hmaidi, A., El Ouali, A., Ousmana, H., and Bouchaou, L.: Assessments of groundwater recharge process and residence time using hydrochemical and isotopic tracers under arid climate: Insights from Er-rachidia basin (Central-East Morocco), *Groundw. Sustain. Dev.*, 25, 101145, <https://doi.org/10.1016/j.gsd.2024.101145>, 2024.
- Fu, B. J., Chen, L., and Ma, K.: The effect of land use change on the regional environment in the Yangjuangou catchment in the loess plateau of China, *Acta Geogr. Sin.*, 54, 241–246, <https://doi.org/10.3321/j.issn:0375-5444.1999.03.006>, 1999.
- Fu, B. J., Liu, Y., Lü, Y. H., He, C. S., Zeng, Y., and Wu, B. F.: Assessing the soil erosion control service of ecosystems change in the Loess Plateau of China, *Ecol. Complex.*, 8, 284–293, <https://doi.org/10.1016/j.ecocom.2011.07.003>, 2011.
- Fu, B. J., Wang, S., Liu, Y., Liu, J., Liang, W., and Miao, C.: Hydrogeomorphic ecosystem responses to natural and anthropogenic changes in the Loess Plateau of China, *Annu. Rev. Earth Planet. Sci.*, 45, 223–243, <https://doi.org/10.1146/annurev-earth-063016-020552>, 2017.
- Gates, J. B., Scanlon, B. R., Mu, X. M., and Zhang, L.: Impacts of soil conservation on groundwater recharge in the semi-arid Loess Plateau, China, *Hydrogeol. J.*, 19, 865–875, <https://doi.org/10.1007/s10040-011-0716-3>, 2011.
- Gleeson, T., Befus, K. M., Jasechko, S., Luijendijk, E., and Cardenas, M. B.: The global volume and distribution of modern groundwater, *Nat. Geosci.*, 9, 161–167, <https://doi.org/10.1038/NNGEO2590>, 2016.
- Gumuła-Kawęcka, A., Jaworska-Szulc, B., Szymkiewicz, A., Gorczewska-Langner, W., Pruszkowska-Caceres, M., Angulo Jaramillo, R., and Šimůnek, J.: Estimation of groundwater recharge in a shallow sandy aquifer using unsaturated zone modeling and water table fluctuation method, *J. Hydrol.*, 605, 127283, <https://doi.org/10.1016/j.jhydrol.2021.127283>, 2022.
- He, M. N., Wang, Y. Q., Tong, Y. P., Zhao, Y. L., Qiang, X. K., Song, Y. G., Wang, L., Song, Y., Wang, G. D., and He, C. X.: Evaluation of the environmental effects of intensive land consolidation: A field-based case study of the Chinese Loess Plateau, *Land Use Policy*, 94, 104523, <https://doi.org/10.1016/j.landusepol.2020.104523>, 2020.
- Healy, R. W. and Cook, P. G.: Using groundwater levels to estimate recharge, *Hydrogeol. J.*, 10, 91–109, <https://doi.org/10.1007/s10040-001-0178-0>, 2002.
- Heppner, C. S. and Nimmo, J. R.: A computer program for predicting recharge with a master recession curve, *U.S. Geol. Surv. Sci. Invest. Rep.*, 2005–5172, <https://doi.org/10.3133/sir20055172>, 2005.
- Huang, J., Li, Y., Fu, C., Chen, F., Fu, Q., Dai, A., Shinoda, M., Ma, Z., Guo, W., Li, Z., Zhang, L., Liu, Y., Yu, H., He, Y., Xie, Y., Guan, X., Ji, M., Lin, L., Wang, S., Yan, H., and Wang, G.: Dryland climate change: Recent progress and challenges, *Rev. Geophys.*, 55, 719–778, <https://doi.org/10.1002/2016RG000550>, 2017.
- Huang, L. M. and Shao, M. A.: Advances and perspectives on soil water research in China's Loess Plateau, *Earth-Sci. Rev.*, 199, 102962, <https://doi.org/10.1016/j.earscirev.2019.102962>, 2019.
- Huang, L. M., Wang, Z. W., Pei, Y. W., Zhu, X. C., Jia, X. X., and Shao, M. A.: Adaptive water use strategies of artificially revegetated plants in a water-limited desert: A case study from the Mu Us Sandy Land, *J. Hydrol.*, 644, 132103, <https://doi.org/10.1016/j.jhydrol.2024.132103>, 2024.
- Huang, T. M. and Pang, Z. H.: Estimating groundwater recharge following land-use change using chloride mass balance of soil profiles: a case study at Guyuan and Xifeng in the Loess Plateau of China, *Hydrogeol. J.*, 19, 177–186, <https://doi.org/10.1007/s10040-010-0643-8>, 2011.
- Huang, T. M., Pang, Z. H., and Edmunds, W. M.: Soil profile evolution following land-use change: Implications for groundwater quantity and quality, *Hydrol. Process.*, 27, 1238–1252, <https://doi.org/10.1002/hyp.9302>, 2013.
- Huang, Y. N., Evaristo, J., and Li, Z.: Multiple tracers reveal different groundwater recharge mechanisms in deep loess deposits, *Geoderma*, 353, 204–212, <https://doi.org/10.1016/j.geoderma.2019.06.041>, 2019.
- Jasechko, S. and Perrone, D.: Global groundwater wells at risk of running dry, *Science*, 372, 418–421, <https://doi.org/10.1126/science.abc2755>, 2021.
- Ji, M. Y., Jia, D. B., Hao, Y. S., Liu, T., Yang, L. N., Li, X. Y., Lyu, C. G., and Shang, Z. Q.: Hydrochemical and isotopic characteristics and water transformation relationships in the Zhenglan Banner section of Shandian River Basin, Chin. *J. Appl. Ecol.*, 35, 3149–3156, <https://doi.org/10.13287/j.1001-9332.202410.015>, 2024.
- Ji, Z. X., Ziegler, A. D., and Wang, L.: Reframing gullies as recharge zones in dryland landscapes of the Loess Plateau, China, Zenodo [data set], <https://doi.org/10.5281/zenodo.18596600>, 2026.
- Jia, X. X., Zhu, P., Wei, X. R., Zhu, Y. J., Huang, M. B., Hu, W., Wang, Y. Q., Turkeltaub, T., Binley, A., Horton, R., and Shao,

- M. A.: Bringing ancient loess critical zones into a new era of sustainable development goals, *Earth-Sci. Rev.*, 255, 104852, <https://doi.org/10.1016/j.earscirev.2024.104852>, 2024.
- Jin, Z., Guo, L., Wang, Y. Q., Yu, Y. L., Lin, H., Chen, Y. P., Chu, G. C., Zhang, J., and Zhang, N. P.: Valley reshaping and damming induce water table rise and soil salinization on the Chinese Loess Plateau, *Geoderma*, 339, 115–125, <https://doi.org/10.1016/j.geoderma.2018.12.048>, 2019.
- Kuang, X. X., Luo, X., Jiao, J. J., Liang, S. H., Zhang, X. L., Li, H. L., and Liu, J. G.: Using stable isotopes of surface water and groundwater to quantify moisture sources across the Yellow River source region, *Hydrol. Process.*, 33, 1835–1850, <https://doi.org/10.1002/hyp.13441>, 2019.
- Kumar, A., Sanyal, P., and Agrawal, S.: Spatial distribution of $\delta^{18}\text{O}$ values in river water in the Ganga River Basin: insight into the hydrological processes, *J. Hydrol.*, 571, 225–234, <https://doi.org/10.1016/j.jhydrol.2019.01.044>, 2019.
- Lai, J. S., Zou, Y., Zhang, J. L., and Peres-Neto, P. R.: Generalizing hierarchical and variation partitioning in multiple regression and canonical analyses using the rdacca.hp R package, *Methods Ecol. Evol.*, 13, 782–788, <https://doi.org/10.1111/2041-210X.13800>, 2022.
- Lamontagne, S., Kirby, J., and Johnston, C.: Groundwater-surface water connectivity in a chain of ponds semiarid river, *Hydrol. Process.*, 35, e14129, <https://doi.org/10.1002/hyp.14129>, 2021.
- Letz, O., Siebner, H., Avrahamov, N., Egozi, R., Eshel, G., and Dahan, O.: The impact of geomorphology on groundwater recharge in a semi-arid mountainous area, *J. Hydrol.*, 603, 127029, <https://doi.org/10.1016/j.jhydrol.2021.127029>, 2021.
- Li, H., Xiang, W., Si, B. C., Min, M., Miao, C. H., and Jin, J. J.: Quantifying recharge mechanisms in low-hilly areas of a loess region: Implications for the quantity and quality of groundwater, *J. Hydrol.*, 643, 131982, <https://doi.org/10.1016/j.jhydrol.2024.131982>, 2024a.
- Li, H. X., Han, S. B., Wu, X., Wang, S., Liu, W. P., Ma, T., Zhang, M. N., Wei, Y. T., Yuan, F. Q., Yuan, L., Li, F. C., Wu, B., Wang, Y. S., Zhao, M. M., Yang, H. W., and Wei, S. B.: Distribution, characteristics and influencing factors of fresh groundwater resources in the Loess Plateau, China, *China Geol.*, 4, 509–526, <https://doi.org/10.31035/cg2021057>, 2021.
- Li, M. Y., Xie, Y. Q., Dong, Y. H., Wang, L. H., and Zhang, Z. Y.: Review: Recent progress on groundwater recharge research in arid and semiarid areas of China, *Hydrogeol. J.*, 32, 9–30, <https://doi.org/10.1007/s10040-023-02656-z>, 2024b.
- Li, Y. S.: Effects of forest on water circle on the Loess Plateau, *J. Nat. Resour.*, 16, 427–432, <https://doi.org/10.11849/zrzyxb.2001.05.005>, 2001.
- Li, Y. R., Shi, W. H., Aydin, A., Beroya-Eitner, M. A., and Gao, G. H.: Loess genesis and worldwide distribution, *Earth-Sci. Rev.*, 201, 102947, <https://doi.org/10.1016/j.earscirev.2019.102947>, 2020.
- Li, Z., Chen, X., Liu, W. Z., and Si, B. C.: Determination of groundwater recharge mechanism in the deep loessial unsaturated zone by environmental tracers, *Sci. Total Environ.*, 586, 827–835, <https://doi.org/10.1016/j.scitotenv.2017.02.061>, 2017.
- Li, Z., Coles, A. E., and Xiao, J.: Groundwater and streamflow sources in China's Loess Plateau on catchment scale, *Catena*, 181, 104075, <https://doi.org/10.1016/j.catena.2019.104075>, 2019.
- Lian, H. S., Yen, H., Yu, K., Zou, J. Y., and Liu, C. X.: Groundwater pollution becomes new constraint after watershed-scale water quality restoration, *J. Hydrol.*, 661, 133558, <https://doi.org/10.1016/j.jhydrol.2025.133558>, 2025.
- Liang, W., Bai, D., Wang, F. Y., Fu, B. J., Yan, J. P., Wang, S., Yang, Y. T., Long, D., and Feng, M. Q.: Quantifying the impacts of climate change and ecological restoration on streamflow changes based on a Budyko hydrological model in China's Loess Plateau, *Water Resour. Res.*, 51, 6500–6519, <https://doi.org/10.1002/2014WR016589>, 2015.
- Liang, X. J., Chi, B. M., Wang, W. K., Gong, H. L., Wang, F. G., Gu, H. B., and Jiang, J. Y. (Eds.): *Applied hydrogeology*, 4th edn., Science Press, Beijing, China, 326 pp., ISBN 9787030487650, 2016.
- Liu, T. S. (Eds.): *Loess and the environment*, Science Press, Beijing, China, 481 pp., ISBN 130312999, 1985.
- Liu, X., Song, X. F., Zhang, Y. H., Xia, J., Zhang, X. C., Yu, J. J., Long, D., Li, F. D., and Zhang, B.: Spatio-temporal variations of $\delta^2\text{H}$ and $\delta^{18}\text{O}$ in precipitation and shallow groundwater in the Hilly Loess Region of the Loess Plateau, China, *Environ. Earth Sci.*, 63, 1105–1118, <https://doi.org/10.1007/s12665-010-0785-y>, 2011.
- Liu, Y. S. and Li, Y.: Engineering philosophy and design scheme of gully land consolidation in Loess Plateau, *Trans. Chin. Soc. Agric. Eng.*, 33, 1–9, <https://doi.org/10.11975/j.issn.1002-6819.2017.10.001>, 2017.
- Liu, Y. S., Chen, Z., Li, Y., Feng, W., and Cao, Z.: The planting technology and industrial development prospects of forage rape in the loess hilly area: A case study of newly-increased cultivated land through gully land consolidation in Yan'an, Shaanxi Province, *J. Nat. Resour.*, 32, 2065–2074, <https://doi.org/10.11849/zrzyxb.20161142>, 2017.
- Liu, Y. Z.: Source analysis of precipitation chemical components on the Loess Plateau based on hydrogen and oxygen stable isotopes, Master thesis, Northwest A&F University, Yangling, China, <https://doi.org/10.27409/d.cnki.gxbnu.2024.001528>, 2024.
- Lu, Y. W.: Study on typical hydrological characteristics of the vadose zone and spatiotemporal evolution of potential groundwater recharge in the Chinese Loess Plateau, Ph.D. thesis, Northwest A&F University, Yangling, China, <https://doi.org/10.27409/d.cnki.gxbnu.2020.001395>, 2020.
- Lupi, L., Bertrand, L., Monferrán, M. V., Amé, M. V., and Diaz, M. del P.: Multilevel and structural equation modeling approach to identify spatiotemporal patterns and source characterization of metals and metalloids in surface water and sediment of the Ctalamochita River in Pampa region, Argentina, *J. Hydrol.*, 572, 403–413, <https://doi.org/10.1016/j.jhydrol.2019.03.019>, 2019.
- Manna, F., Murray, S., Abbey, D., Martin, P., Cherry, J., and Parker, B.: Spatial and temporal variability of groundwater recharge in a sandstone aquifer in a semiarid region, *Hydrol. Earth Syst. Sci.*, 23, 2187–2205, <https://doi.org/10.5194/hess-23-2187-2019>, 2019.
- Medici, G., Munn, J. D., and Parker, B. L.: Delineating aquitard characteristics within a Silurian dolostone aquifer using high-density hydraulic head and fracture datasets, *Hydrogeol. J.*, 32, 1663–1691, <https://doi.org/10.1007/s10040-024-02824-9>, 2024.
- Meles, M. B., Bradford, S., Casillas-Trasvina, A., Chen, L., Osterman, G., Hatch, T., Ajami, H., Crompton, O., Levers, L., and Kisekka, I.: Uncovering the gaps in managed aquifer

- recharge for sustainable groundwater management: A focus on hillslopes and mountains, *J. Hydrol.*, 639, 131615, <https://doi.org/10.1016/j.jhydrol.2024.131615>, 2024.
- Nachabe, M. H.: Analytical expressions for transient specific yield and shallow water table drainage, *Water Resour. Res.*, 38, 11–17, <https://doi.org/10.1029/2001WR001071>, 2002.
- Nicholson, S. E. (Eds.): *Dryland Climatology*, Cambridge University Press, Cambridge, UK, 516 pp., <https://doi.org/10.1017/CBO9780511973840>, 2011.
- Obuobie, E., Diekkruuger, B., Agyekum, W., and Agodzo, S.: Groundwater level monitoring and recharge estimation in the White Volta River basin of Ghana, *J. Afr. Earth Sci.*, 71–72, 80–86, <https://doi.org/10.1016/j.jafrearsci.2012.06.005>, 2012.
- Owuor, S. O., Butterbach-Bahl, K., Guzha, A. C., Rufino, M. C., Pelster, D. E., Díaz-Pinés, E., and Breuer, L.: Groundwater recharge rates and surface runoff response to land use and land cover changes in semi-arid environments, *Ecol. Process.*, 5, 16, <https://doi.org/10.1186/s13717-016-0060-6>, 2016.
- Pécsi, M.: Loess is not just the accumulation of dust, *Quat. Int.*, 7–8, 1–21, [https://doi.org/10.1016/1040-6182\(90\)90034-2](https://doi.org/10.1016/1040-6182(90)90034-2), 1990.
- Qiao, J. B., Zhu, Y. J., Jia, X. X., Huang, L. M., and Shao, M. A.: Spatial variability of soil water for the entire profile in the critical zone of the Loess Plateau, *Adv. Water Sci.*, 28, 515–522, <https://doi.org/10.14042/j.cnki.32.1309.2017.04.005>, 2017.
- Qu, S., Zhao, Y. Z., Li, M. H., Ren, X. H., Wang, C. Y., Yang, X., Hao, Y. L., Dong, S. G., and Yu, R. H.: Unveiling sources and fate of sulfate in lake-groundwater system combined Bayesian isotope mixing model with radon mass balance model, *Water Res.*, 282, 123648, <https://doi.org/10.1016/j.watres.2025.123648>, 2025.
- Salek, M., Levison, J., Parker, B., and Gharabaghi, B.: CAD-DRASTIC: chloride application density combined with DRASTIC for assessing groundwater vulnerability to road salt application, *Hydrogeol. J.*, 26, 2379–2393, <https://doi.org/10.1007/s10040-018-1801-7>, 2018.
- Scanlon, B. R., Healy, R. W., and Cook, P. G.: Choosing appropriate techniques for quantifying groundwater recharge, *Hydrogeol. J.*, 10, 18–39, <https://doi.org/10.1007/s10040-001-0176-2>, 2002.
- Shah, N. and Ross, M.: Variability in specific yield under shallow water table conditions, *J. Hydrol. Eng.*, 14, 1290–1298, [https://doi.org/10.1061/\(ASCE\)HE.1943-5584.0000121](https://doi.org/10.1061/(ASCE)HE.1943-5584.0000121), 2009.
- Shi, H. and Shao, M. A.: Soil and water loss from the Loess Plateau in China, *J. Arid Environ.*, 45, 9–20, <https://doi.org/10.1006/jare.1999.0618>, 2000.
- Tan, H. B., Wen, X. W., Rao, W. B., Bradd, J., and Huang, J. Z.: Temporal variation of stable isotopes in a precipitation-groundwater system: implications for determining the mechanism of groundwater recharge in high mountain hills of the Loess Plateau, China, *Hydrol. Process.*, 30, 1491–1505, <https://doi.org/10.1002/hyp.10729>, 2016.
- Tan, H. B., Liu, Z. H., Rao, W. B., Jin, B., and Zhang, Y. D.: Understanding recharge in soil-groundwater systems in high loess hills on the Loess Plateau using isotopic data, *Catena*, 156, 18–29, <https://doi.org/10.1016/j.catena.2017.03.022>, 2017.
- Tetzlaff, D., Seibert, J., McGuire, K. J., Laudon, H., Burns, D. A., Dunn, S. M., and Soulsby, C.: How does landscape structure influence catchment transit time across different geomorphic provinces?, *Hydrol. Process.*, 23, 945–953, <https://doi.org/10.1002/hyp.7240>, 2009.
- Tooth, S.: Arid geomorphology: Changing perspectives on timescales of change, *Prog. Phys. Geogr.*, 36, 262–284, <https://doi.org/10.1177/0309133311417943>, 2012.
- Wan, H. and Liu, W. G.: An isotope study ($\delta^{18}\text{O}$ and $\delta^2\text{H}$) of water movements on the Loess Plateau of China in arid and semiarid climates, *Ecol. Eng.*, 93, 226–233, <https://doi.org/10.1016/j.ecoleng.2016.05.039>, 2016.
- Wang, L., Shao, M., Wang, Q. J., and Gale, W. J.: Historical changes in the environment of the Chinese Loess Plateau, *Environ. Sci. Policy*, 9, 675–684, <https://doi.org/10.1016/j.envsci.2006.08.003>, 2006.
- Wang, W. Z., Sun, J. N., Xia, Y., and Li, Z.: Identifying hydraulic connectivity among the vadose zone, unconfined and confined aquifers in the thick loess deposits using multiple tracers, *J. Hydrol.*, 626, 130339, <https://doi.org/10.1016/j.jhydrol.2023.130339>, 2023.
- Wang, W. Z., Xia, Y., Sun, J. N., Liu, Y. Z., Li, P. Y., Han, F. P., and Li, Z.: Uncertainties in physical and tracer methods in actual groundwater recharge estimation in the thick loess deposits of China, *J. Hydrol.*, 634, 131127, <https://doi.org/10.1016/j.jhydrol.2024.131127>, 2024.
- Wang, Y. Q., Shao, M. A., Sun, H., Fu, Z. H., Fan, J., Hu, W., and Fang, L. C.: Response of deep soil drought to precipitation, land use and topography across a semi-arid watershed, *Agric. For. Meteorol.*, 282–283, 107866, <https://doi.org/10.1016/j.agrformet.2019.107866>, 2020.
- Wu, M. L. (Eds.): *Structural Equation Modeling – Operation and Application of AMOS*, 2nd edn., Chongqing University Press, Chongqing, China, 517 pp., ISBN 9787562457206, 2010.
- Xiang, W.: Study on soil evaporation and groundwater recharge based on stable isotopes in the Loess Plateau at regional scale, Ph.D. thesis, Northwest A&F University, Yangling, China, <https://doi.org/10.27409/d.cnki.gxbnu.2021.000025>, 2021.
- Xiang, W., Si, B. C., Biswas, A., and Li, Z.: Quantifying dual recharge mechanisms in deep unsaturated zone of Chinese Loess Plateau using stable isotopes, *Geoderma*, 337, 773–781, <https://doi.org/10.1016/j.geoderma.2018.10.006>, 2019.
- Xie, T. T., Zhao, H. J., Chen, G. K., and Lin, H. H.: Land Use Patterns and River Nitrate Dynamics in Karst Regions: Insights from High-Resolution Sentinel-2 Imagery and Partial Least Squares Structural Equation Modeling Analysis, *Environ. Eng. Sci.*, 42, 203–215, <https://doi.org/10.1089/ees.2024.0272>, 2025.
- Xu, P., Weng, B. S., Gong, X. Y., Xia, K. B., Yan, D. H., and Wang, H.: Estimation of shallow groundwater recharge in central Qinghai-Tibet Plateau by combining unsaturated zone simulation and improved water table fluctuation method, *J. Hydrol.*, 630, 130689, <https://doi.org/10.1016/j.jhydrol.2024.130689>, 2024.
- Xu, Y. and Beekman, H. E.: Review: Groundwater recharge estimation in arid and semi-arid southern Africa, *Hydrogeol. J.*, 27, 929–943, <https://doi.org/10.1007/s10040-018-1898-8>, 2019.
- Xu, Z. Y., Zhao, Y. J., and Chen, J. J.: Research of fractured efficacy on mechanisms governing water flow in unsaturated loess, *J. Changchun Univ. Earth Sci.*, 23, 326–329, 1993.
- Xue, S. B., Li, P., Cui, Z. W., and Li, Z. B.: The influence of different check dam configurations on the downstream river topography and water-sediment relationship, *J. Hydrol.*, 656, 133046, <https://doi.org/10.1016/j.jhydrol.2025.133046>, 2025.
- Yang, N. and Wang, G. C.: Spatial variation of water stable isotopes of multiple rivers in southeastern

- Qaidam Basin, northeast Qinghai-Tibetan Plateau: Insights into hydrologic cycle, *J. Hydrol.*, 628, 130464, <https://doi.org/10.1016/j.jhydrol.2023.130464>, 2023.
- Yu, L. L., Ji, Z. X., and Wang, L.: Characteristics of Perched Water Recharge in the Dam Land of Yangjuangou Small Watershed on the Loess Plateau, *Acta Pedol. Sin.*, 62, 983–997, <https://doi.org/10.11766/trxb202404290178>, 2025.
- Yu, Y. L., Jin, Z., Chu, G. C., Zhang, J., Wang, Y. Q., and Zhao, Y. L.: Effects of valley reshaping and damming on surface and groundwater nitrate on the Chinese Loess Plateau, *J. Hydrol.*, 584, 124702, <https://doi.org/10.1016/j.jhydrol.2020.124702>, 2020.
- Zhang, H., Xu, Y. X., and Kanyerere, T.: A review of the managed aquifer recharge: Historical development, current situation and perspectives, *Phys. Chem. Earth, Parts A/B/C*, 118–119, 102887, <https://doi.org/10.1016/j.pce.2020.102887>, 2020.
- Zhang, J., Chen, H. S., Fu, Z. Y., Wang, F., and Wang, K. L.: Towards hydrological connectivity in the karst hillslope critical zone: Insight from using water isotope signals, *J. Hydrol.*, 617, 128926, <https://doi.org/10.1016/j.jhydrol.2022.128926>, 2023.
- Zhang, Y. H. and Wu, Y. Q.: Oxygen and Hydrogen Isotopes in Precipitation in Heihe River Basin, China, *J. Glaciol. Geocryol.*, 31, 34–39, <https://doi.org/10.7522/j.issn.1000-0240.2009.0005>, 2009.
- Zhao, Y. and Wang, L.: Determination of groundwater recharge processes and evaluation of the “two water worlds” hypothesis at a check dam on the Loess Plateau, *J. Hydrol.*, 595, 125989, <https://doi.org/10.1016/j.jhydrol.2021.125989>, 2021.
- Zhao, Y. L., Wang, Y. Q., Sun, H., Lin, H., Jin, Z., He, M. N., Yu, Y. L., Zhou, W. J., and An, Z. S.: Intensive land restoration profoundly alters the spatial and seasonal patterns of deep soil water storage at watershed scales, *Agric. Ecosyst. Environ.*, 280, 129–141, <https://doi.org/10.1016/j.agee.2019.04.028>, 2019.
- Zhao, Y. L., Wang, Y. Q., Zhou, J. X., Qi, L. J., and Zhang, P. P.: Spatiotemporal variation and controlling factors of dried soil layers in a semi-humid catchment and relevant land use management implications, *Catena*, 240, 107973, <https://doi.org/10.1016/j.catena.2024.107973>, 2024.
- Zhu, Y. J., Jia, X. X., and Shao, M. A.: Loess thickness variations across the loess plateau of China, *Surv. Geophys.*, 39, 715–727, <https://doi.org/10.1007/s10712-018-9462-6>, 2018.